Zootaxa 4365 (2): 149–172
http://www.mapress.com/j/zt/

Article

ISSN 1175-5326 (print edition)
ZOOTAXA
ISSN 1175-5334 (online edition)

https://doi.org/10.11646/zootaxa.4365.2.3
http://zoobank.org/urn:lsid:zoobank.org:pub:EC3AA081-4FC9-498F-98CF-FAF66AA7E025

A new species of *Plestiodon* (Squamata: Scincidae) from the Balsas Basin, Mexico

CARLOS J. PAVÓN-VÁZQUEZ[1, 4], ADRIÁN NIETO-MONTES DE OCA[1, 5],
ANDRÉS A. MENDOZA-HERNÁNDEZ[1], ERIC CENTENERO-ALCALÁ[2],
SAMUEL A. SANTA CRUZ-PADILLA[3] & VÍCTOR H. JIMÉNEZ-ARCOS[2]

[1]*Museo de Zoología and Departamento de Biología Evolutiva, Facultad de Ciencias, Universidad Nacional Autónoma de México, Ciudad Universitaria, México, Ciudad de México 04510, Mexico*

[2]*Laboratorio de Ecología, UBIPRO, FES Iztacala, Universidad Nacional Autónoma de México, Av. de los Barrios No. 1, Los Reyes Ixtacala, Tlalnepantla, Estado de México 54090, Mexico*

[3]*Naturam Sequi A.C., 16 de Septiembre #43, Col. Cd. de los Niños, Naucalpan de Juárez, Estado de México 53450, Mexico*

[4]*Current address: Division of Ecology and Evolution, Research School of Biology, Australian National University, Canberra, ACT 2601, Australia*

[5]*Corresponding author. E-mail: anietomontesdeoca@me.com*

Abstract

We describe a new species of *Plestiodon* in the *P. brevirostris* group from the Balsas Basin in central Mexico. It is distinguished from the other species in the group by the following combination of traits: supraoculars four; interparietal enclosed posteriorly by parietals; primary temporal present; seventh supralabial usually contacting upper secondary temporal; longitudinal dorsal scale rows around midbody 23–26; Toe-IV lamellae 13–15; limbs not overlapping when adpressed against body; dorsolateral light line extending posteriorly to level of posterior end of anterior fourth of body or beyond; light median line absent in all growth stages; primary lateral dark lines separated medially by six dorsal scale rows and upper half of adjacent row on each side at level of midbody; lower secondary dark line faint at level of neck; and light coloration of supralabials extending ventrally to lip border. Analyses based on DNA sequences of three loci support the distinctiveness of the new species, as well as its sister species relationship with *P. ochoterenae*. The Environmental Vulnerability Score of the new species places it in the high vulnerability category.

Resumen

Describimos una nueva especie de *Plestiodon* en el grupo *P. brevirostris* de la Cuenca del Balsas en México central. Se distingue de las demás especies del grupo por poseer la siguiente combinación de características: supraoculares cuatro; interparietal encerrada posteriormente por las parietales; temporal primaria presente; séptima supralabial usualmente en contacto con la temporal secundaria superior; hileras longitudinales de escamas dorsales alrededor de la mitad del cuerpo 23–26; laminillas bajo Dedo del Pie-IV 13–15; extremidades que no se superponen al flexionarse contra el cuerpo; línea dorsolateral clara extendiéndose posteriormente hasta el extremo posterior del cuarto anterior del cuerpo o más allá; línea clara media ausente en todos los estadíos de crecimiento; líneas primarias oscuras separadas medialmente por seis hileras de escamas dorsales y mitad superior de la hilera adyacente en cada lado al nivel de la mitad del cuerpo; línea oscura secundaria tenue al nivel del cuello; y coloración clara de las supralabiales extendiéndose hasta el borde del labio. Análisis basados en secuencias de DNA de tres loci apoyan la separación de la nueva especie, así como su relación de especies hermanas con *P. ochoterenae*. La Puntuación de Vulnerabilidad Ambiental de la nueva especie la coloca en la categoría de vulnerabilidad alta.

Key words: Environmental Vulnerability Score, Guerrero, Morelos, Oaxaca, Puebla, Skink, Systematics, Taxonomy

Introduction

The skink genus *Plestiodon* is a monophyletic taxon with a disjunct distribution in Asia (including islands),

Accepted by C. Siler: 31 Oct. 2017; published: 18 Dec. 2017

Bermuda, and North and Central America (Brandley *et al*. 2011, 2012). It includes 49 described species (Uetz 2016; Kurita *et al*. 2017 a, b), which collectively occupy a great variety of vegetation types ranging from xeric habitats in high plateaus to tropical evergreen forest (Griffith 1991; Brandley *et al*. 2012). The *P. brevirostris* group was defined originally by Taylor (1935), who recognized six species: *P. brevirostris* (Günther), *P. indubitus* (Taylor), *P. dugesii* (Thominot), *P. colimensis* (Taylor), *P. dicei* (Ruthven & Gaige), and *P. ochoterenae* (Taylor). After a series of taxonomic modifications (summarized by Feria-Ortiz *et. al.* 2011), Dixon (1969) redefined the group to include five species: *P. brevirostris*, *P. colimensis*, *P. copei* (Taylor), *P. dugesii*, and *P. ochoterenae*. Additionally, he regarded *P. brevirostris* as polytypic, including the following subspecies: *P. b. brevirostris*, *P. b. bilineatus* (Tanner), *P. b. dicei*, *P. b. indubitus*, and *P. b. pineus* (Axtell). Later, Robinson (1979) increased the number of species in the group to seven, with the inclusion of *P. parviauriculatus* (Taylor) and *P. parvulus* (Taylor). Furthermore, molecular analyses performed by Brandley *et al*. (2011, 2012) and Feria-Ortiz *et al*. (2011) revealed some necessary modifications to the composition of the group: the inclusion of *P. lynxe* (Wiegmann) and *P. sumichrasti* (Cope) within the group (subsequently supported by Pyron *et al*. 2013 and Bryson *et al*. 2017), the elevation to specific status of the former subspecies *P. b. brevirostris*, *P. b. bilineatus*, *P. b. dicei*, and *P. b. indubitus* (with *P. b. pineus* tentatively placed in the synonymy of *P. b. dicei*), and the inclusion of an undescribed species similar to *P. indubitus* from Colima and Jalisco in west-central Mexico (Feria-Ortiz *et al*. 2011). Additionally, *P. nietoi* Feria-Ortiz & García-Vázquez was recently described in the group (Feria-Ortiz & García-Vázquez 2012). Thus, as currently understood, the *P. brevirostris* group is composed of 13 described species (*P. brevirostris*, *P. bilineatus*, *P. colimensis*, *P. copei*, *P. dicei*, *P. dugesii*, *P. indubitus*, *P. lynxe* [with subspecies *P. l. lynxe* and *P. l. belli* Gray], *P. nietoi*, *P. ochoterenae*, *P. parviauriculatus*, *P. parvulus*, and *P. sumichrasti*) and the undescribed species from west-central Mexico (hereafter *Plestiodon* sp. Colima-Jalisco).

Dixon (1969) suggested that some specimens of *Plestiodon* from Morelos might represent intergrades between *P. brevirostris brevirostris* (= *P. brevirostris*) and *P. b. indubitus* (= *P. indubitus*) based on their possession of a unique set of traits: interparietal scale enclosed posteriorly by the parietals accompanied by a faint lateral light line on the neck, or a non-enclosed interparietal without a lateral light line on the neck. One of these specimens came from 5 mi E Cuernavaca, at ca. 1500 m elevation, in the Balsas Basin. The Balsas Basin biogeographic province in central Mexico is constituted by a low elevation drainage (below 2000 m) with an east-west direction that separates two mountainous provinces, the Transmexican Volcanic Belt and the Sierra Madre del Sur (Fig. 1; Morrone 2014). The region is relatively dry and tropical deciduous forest is the dominant vegetation type, differing from the comparatively humid surrounding mountains (Rzedowski 1983). Feria-Ortiz *et al*. (2011) reported a specimen of *P. brevirostris* from Acatlipa, Morelos, also in the Balsas Basin, and noted that it differed from most of the other specimens assigned to this species by having the parietals in medial contact with each other posteriorly (enclosing the interparietal posteriorly) and by lacking a light line on the 5th and 6th supralabials. Feria-Ortiz & García-Vázquez (2012) assigned this specimen to *P. indubitus*; however, specimens of *P. indubitus* have a light line on the 5th and 6th supralabials. Thus, the assigment of the known specimens of *Plestiodon* from the Balsas Basin to described species is problematical.

Based on the examination of additional specimens from the Balsas Basin and molecular analyses of the *P. brevirostris* group, we show that the populations of *Plestiodon* from the Balsas Basin represent a novel species and provide a description and illustration of this species.

Materials and methods

Morphology. One of us (CJPV) examined 14 specimens of *Plestiodon* from the Balsas Basin and 351 specimens of seven species in the *P. brevirostris* group (number of specimens of each taxon in parentheses): *P. brevirostris* (122), *P. copei* (62), *P. indubitus* (33), *P. lynxe lynxe* (92), *P. nietoi* (14), *P. ochoterenae* (7), and *P. sumichrasti* (21). Nomenclature of scales follows Taylor (1935), except for the substitution of upper and lower labials for supralabials and infralabials, respectively. Nomenclature of coloration traits follows Dixon (1969). Our character selection was based on Feria Ortiz (2011), Feria-Ortiz *et al*. (2011), Pavón Vázquez (2015), and references included therein. We recorded five characters with diagnostic value on all the specimens: (1) interparietal (in contact with nuchals or enclosed posteriorly by parietals), (2) light coloration of sixth and seventh supralabials (separated from lip border, extending to lip border and showing scattered dark markings, or extending to lip border and immaculate), (3) median light line (present or absent), (4) number of dorsal scale rows separating primary

lateral dark lines medially, and (5) lateral light line at level of midneck (continuous or not and discernible or not from light ventral coloration). Other 28 characters (Supplementary Table 1) were recorded in all the specimens from the Balsas Basin. The comparison with the other members of the *P. brevirostris* group was based on the specimens examined and information in Feria Ortiz (2011) and Feria Ortiz *et al*. (2011) for *P. bilineatus*, *P. dicei*, *P. dugesii*, *P. parvulus*, and *Plestiodon* sp. Colima-Jalisco; Peters (1954), Webb (1959), and Feria Ortiz (2011) for *P. colimensis*; Webb (1968) and Feria Ortiz (2011) for *P. l. belli*; and Robinson (1979) for *P. parviauriculatus*. We performed scale counts with the aid of a dissecting microscope. We scored bilateral characters on both sides. Sample sizes for bilateral characters used in the diagnosis equal the number of times each character was scored, not the number of specimens. When the condition of a given character was not identical on both sides, the conditions on the left and right sides are given, in that order, separated by a slash (/). Measurements were taken with digital calipers or an ocular micrometer to the nearest 0.1 mm. We measured head width at its widest point (between angles of jaws), head length from the tip of the snout to the posterior end of the ear opening, and trunk length between the posterior and anterior points of insertion of the fore-limbs and hind limbs, respectively. All scale dimensions were measured at their maximum. Color codes and names (in parentheses) follow Köhler (2012). Acronyms for herpetological collections follow Sabaj (2016), except for MZFC-HE (Museo de Zoología "Alfonso L. Herrera," Facultad de Ciencias, Universidad Nacional Autónoma de México, Ciudad de México, México).

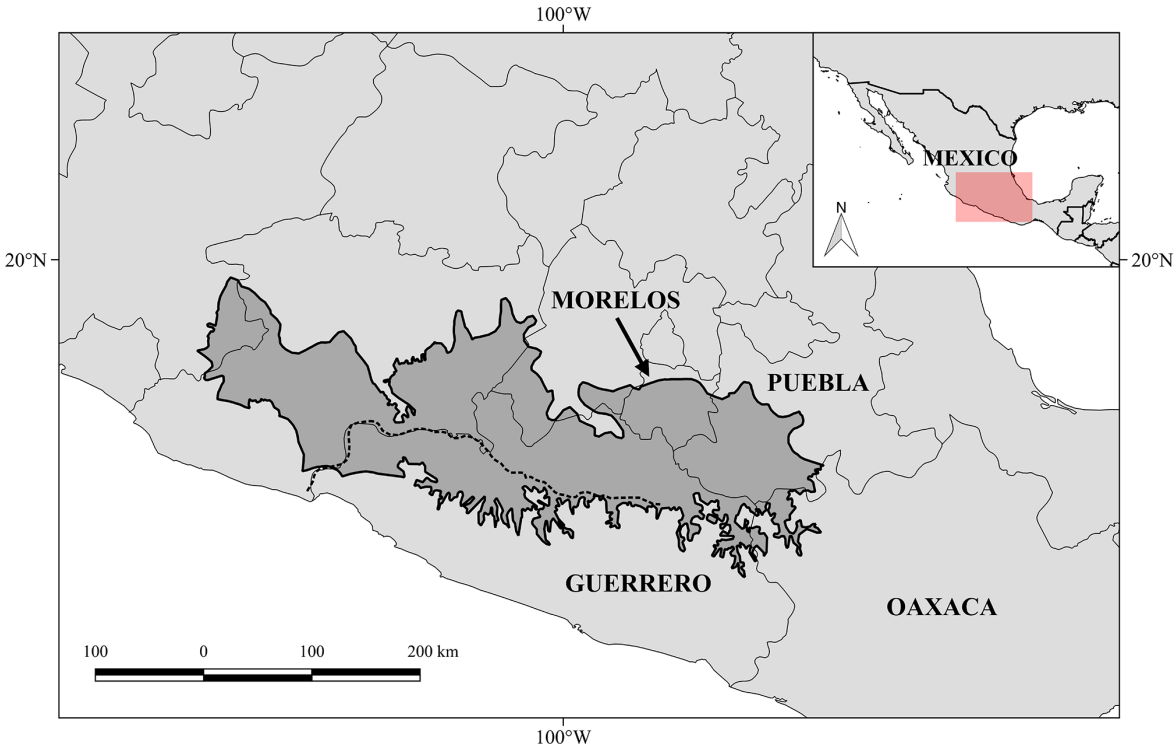

FIGURE 1. Geographic location of the Balsas Basin biogeographic province. Narrow continuous lines represent state limits. The dashed line represents the main stem of the Balsas River.

Molecular sampling. We obtained sequences of a mtDNA fragment including partial sequences of the 16S ribosomal RNA (*16S*) and tRNA-Met genes, and complete sequences of the genes coding for the NADH dehydrogenase subunit 1 (*ND1*), tRNA-Ile, tRNA-Leu, and tRNA-Gln for seven specimens from the Balsas Basin (sequences of two specimens were incomplete). Additionally, we sequenced a fragment each of the nuclear genes coding for the megakaryoblastic leukaemia 1 (*MKL1*) and RNA fingerprint 35 (*R35*) proteins for four specimens from the Balsas Basin and six specimens of other species of *Plestiodon*. Additional sequences were downloaded from GenBank (GB). A reference number was assigned to each sequence and the GB accession number and locality data for each voucher are given in Supplementary Table 2. We extracted the genomic DNA from ethanol-preserved tissues with the use of the standard phenol-chloroform method (Hillis *et al*. 1996). Amplification was accomplished using the polymerase chain reaction (PCR) with the primers 16aR2 (Reeder 2003) and tMET (Leaché & Reeder 2002) for the mtDNA fragment, MKL1_f1 and MKL1_r2 (Townsend *et al*. 2008) for *MKL1*, and R35-F and R35-R (Brandley *et al*. 2011) for *R35*. PCR cycle parameters for the mtDNA fragment were: an initial denaturation cycle at 94°C for 5 min,

followed by 40 cycles of denaturation at 94°C for 30 s, primer annealing at 48°C for 30 s, and extension at 72°C for 105 s; and a final extension cycle at 72°C for 10 min. PCR for the nuclear loci followed a "Touch-Down" protocol with the following characteristics: an initial denaturation cycle at 94°C for 1 min followed by five cycles of denaturation at 94°C for 30s, pairing of primers at 61°C for 30s, and extension at 68°C for 1:30 min. The conditions of the latter five cycles were repeated five times lowering the pairing temperature by two degrees each time reaching 57°C. The protocol concluded with 25 cycles of denaturation at 94°C for 30s, pairing of primers at 50°C for 30s, and extension at 68°C for 1:30 min. DNA templates were sequenced with an ABI 3730xl (Applied Biosystems, Inc.) automated DNA sequencer. The primers used for sequencing were ND1-INTR2 (Schmitz *et al*. 2005) and F4-skink (5'-TDGCMCAAACHATYTCMTAMGA-3') for the mtDNA fragment and the same primers used for amplification in the case of the nuclear loci.

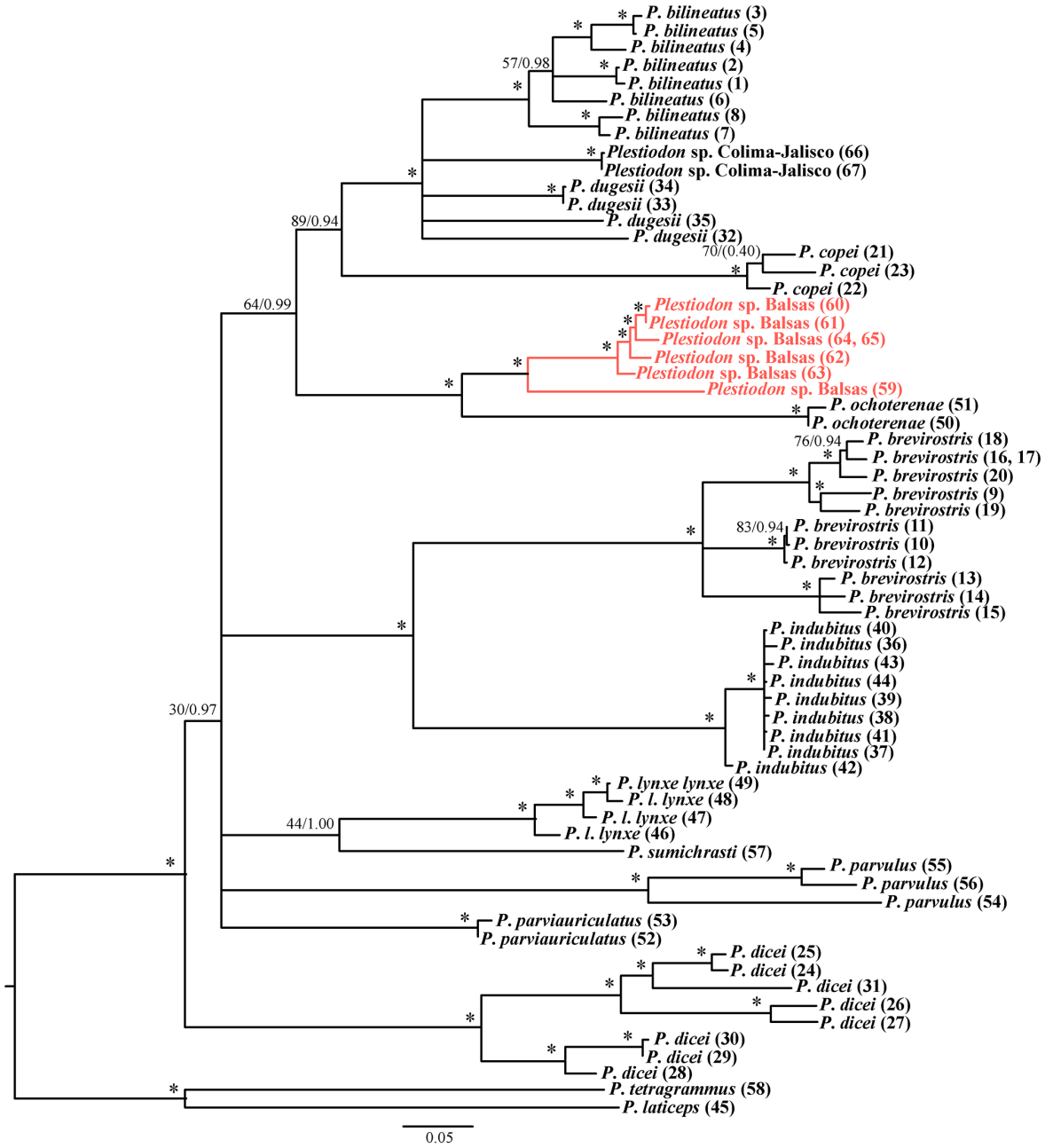

FIGURE 2. Phylogenetic hypothesis of the *Plestiodon brevirostris* group based on mtDNA data. Asterisks above branches indicate that they are strongly supported in both the maximum likelihood and Bayesian analyses (BS ≥ 70, PP ≥ 0.95). Numbers above branches indicate BS and PP values, in that order, for clades in which one of the two is non-significant. The PP of a clade within *P. copei* found in the maximum likelihood tree but not in the MCC tree is shown in parentheses. Reference numbers for each sample are shown in parentheses next to each taxon name.

TABLE 1. Selected characters in the sample of *Plestiodon* from the Balsas Basin and the geographically closest species in the *P. brevirostris* group. Variation based on specimens examined. Sample size in parentheses. Characters abbreviated as follows: (1) Interparietal enclosed posteriorly by parietals (%); (2) coloration of sixth and seventh supralabials (%): (2A) light coloration separated from lip border by dark line, (2B) light coloration extending to lip border, scattered dark speckles on lip border, (2C) light coloration extending to lip border, dark speckles absent on lip border; (3) median light line; (4) dorsal scale rows separating primary lateral dark lines medially (%): (4A) four and upper halves of adjacent two, fourth dorsal scale row dark, (4B) four and upper halves of adjacent two, upper half of fourth dorsal scale row light, (4C) five and upper halves of adjacent two, (4D) six, (4E) six and upper halves of adjacent two, (4F) seven and upper halves of adjacent two, (4G) eight; (5) condition of lateral light line and lower secondary dark line on neck (%): (5A) lateral light line and lower secondary dark line conspicuous, (5B) lateral light line conspicuous, lower secondary dark line faint, (5C) lines replaced by a series of scales with white anterior edges and centers and black posterior borders, (5D) lateral light line indistinguishable from light ventral coloration, lower secondary dark line absent; and (6) geographic distribution.

Character	***Plestiodon* sp. Balsas (14)**	***P. brevirostris* (122)**	***P. copei* (62)**	***P. indubitus* (33)**	***P. lynxe lynxe* (92)**	***P. nietoi* (14)**	***P. ochoterenae* (7)**	***P. sumichrasti* (21)**
1	100	17.36	3.23 (specimens with interparietal damaged)	93.94	5.26	100	14.29	14.29
2								
A	0	76.23	87.1	100	1.09	92.86	0	47.62 (juvenile)
B	0	6.56	12.9	0	5.43	7.14	0	19.05 (juvenile)
C	100	17.21	0	0	93.48	0	100	33.33
3	Absent	Absent	Absent	Absent	Present (faint in large adults)	Absent	Absent	Present (faint in large adults)
4								
A	0	52.46	100	0	0	21.43	100	0
B	0	38.52	0	0	8.7	57.14	0	0
C	0	0	0	0	0	0	0	4.76
D	0	0	0	0	0	21.43	0	0
E	100	9.01	0	100	91.3	0	0	85.71
F	0	0	0	0	0	0	0	4.76
G	0	0	0	0	0	0	0	4.76
5								
A	0	98.36	100	9.09	34.78	85.71	14.29	76.19 (juvenile)
B	100	1.64	0	0	32.61	7.14	42.86	14.29
C	0	0	0	90.91	7.61	0	0	0
D	0	0	0	0	25	0	42.86	9.52
6	Balsas Basin in Guerrero, Morelos, Oaxaca, and Puebla (Mexico)	Sierra Madre del Sur in Guerrero and Oaxaca; Transmexican Volcanic Belt, and Sierra Madre Oriental in México, Puebla, Tlaxcala, and Veracruz (Mexico)	Transmexican Volcanic Belt in Ciudad de México, Michoacán, Mexico, Morelos, Puebla, Tlaxcala, and Veracruz (Mexico)	Transmexican Volcanic Belt in Ciudad de México, Guerrero, Mexico, Michoacán, and Morelos (Mexico)	Central Mexican Plateau, northern edge of Transmexican Volcanic Belt, and Sierra Madre Oriental in Guanajuato, Hidalgo, Puebla, Querétaro, San Luis Potosí, Tamaulipas, Tlaxcala, and Veracruz (Mexico)	Sierra Madre del Sur in Guerrero (Mexico)	Sierra Madre del Sur in Guerrero and Oaxaca (Mexico)	Atlantic lowlands from Veracruz, Mexico, southeastward to Guatemala, Belize, and Honduras; apparently disjunct population in northern Yucatán Peninsula

Phylogenetics. We aligned the obtained sequences using the MUSCLE algorithm (Edgar 2004) included in the software MEGA 6.06 (Tamura *et al*. 2013). We optimized the alignment visually and removed regions of ambiguous alignment in the mtDNA dataset. We used PartitionFinder 2.1.1 (Lanfear *et al*. 2016) to determine the best-fitting partition scheme and substitution model for each locus based on the corrected Akaike Information Criterion (AICc). All phylogenetic analyses were conducted in the CIPRES Science Gateway (Miller *et al*. 2010). Sequences of *Plestiodon laticeps* (Schneider) and *P. tetragrammus* Baird, both belonging to the *P. fasciatus* group, were included as outgroups. We performed a partitioned maximum likelihood phylogenetic analysis of the mtDNA matrix in RAxML-HPC 8 (Stamatakis 2014) under the GTRGAMMA model. Support values were obtained by performing 1000 rapid bootstrap replicates. Additionally, we performed a Bayesian analysis of the mtDNA matrix in BEAST 1.8.4 (Drummond *et al*. 2012). We specified a strict clock model for the molecular clock and a coalescent model with constant population size for the tree. Two independent runs were conducted for 300 million generations with sampling every 15,000 generations. We evaluated the results for convergence and sufficient sampling in Tracer 1.6 (Rambaut *et al*. 2014) and combined the trees obtained in each run using LogCombiner 1.8.4 (Drummond *et al*. 2012). The maximum clade credibility (MCC) tree was annotated in TreeAnnotator 1.8.4 (Drummond *et al*. 2012) after specifying a burnin of 10%. Finally, we inferred a species tree in *BEAST as implemented in BEAST 2.4.5 (Bouckaert *et al*. 2014) based on the sequences for the three loci. We only included the individuals for which sequences of the three loci were available. For this analysis, we reconstructed the haplotypes for the diploid loci in PHASE 2.1.1 (Stephens *et al*. 2001; Stephens & Scheet 2005) using the default settings after formatting the sequences in SeqPHASE (Flot 2010). In our mtDNA analyses a sample from the vicinities of Arcelia, Guerrero, in the Balsas Basin, appeared as sister to all the other samples in the mtDNA analyses and is connected to them by a relatively long branch (see below). Additionally, *Plestiodon dugesii* was not monophyletic (see below). Thus, we assigned the sample from Arcelia to its own species, the remaining samples from the Balsas Basin to another, and the samples from each clade of *P. dugesii* to their own species. The specific assignment of the other samples was made following our current understanding of the *P. brevirostris* group (see Introduction). We specified a strict clock prior for the molecular clock and a Yule model for the tree. Two independent runs were conducted for 500 million generations with sampling every 12,500 generations. We processed the results and annotated the MCC the same way as for the Bayesian analysis of the mtDNA. We consider nodes with a bootstrap value (BS) $\geq$ 70 and a posterior probability (PP) $\geq$ 0.95 to be significantly supported (Hillis & Bull 1993; Huelsenbeck & Rannala 2004).

Species delimitation. We evaluated the species limits within the clade containing the samples from the Balsas Basin and *Plestiodon ochoterenae* (see below) with BP&P 3.3 (Yang 2015) based on the mtDNA and phased nDNA sequences. We allowed the topology of the species tree to vary (analysis A11 of Yang 2015) and used the three combinations of priors for the root age and ancestral population size used by Leaché & Fujita (2010). We specified a three-species model as prior, including *P. ochoterenae*, the individual from Arcelia, and the remaining samples from the Balsas Basin. We used algorithm 0 of Yang & Rannala (2010) with = 15. We specified the *BEAST topology as the prior for the species tree. To test if each analysis was getting stuck in models with a certain number of species regardless of the information provided by the data, we conducted two additional sets of analyses randomizing the assignment of sequences (1) between all the species and (2) between the sample from Arcelia and the other samples from the Balsas Basin (Rittmeyer & Austin 2017). All analyses consisted of a burnin period of 10,000 iterations, followed by a post-burnin period of 500,000 iterations sampled every fifth iteration. We ran each analysis twice to confirm consistency between runs.

Environmental Vulnerability Score (EVS). We calculated the EVS of the new species as proposed for Mexican reptiles by Wilson *et al*. (2013). Placing a certain species in one of IUCN's categories requires time-consuming demographic assessments, while the EVS provides a rapid way of evaluating the vulnerability of the taxon that aides in the development of a conservation strategy (Wilson *et al*. 2013). The EVS is the sum of the scores for three scales: extent of geographic distribution, number of vegetation types inhabited, and degree of human persecution (Wilson *et al*. 2013). These variables can usually be scored or inferred upon the collecting and description of a new species (Wilson *et al*. 2013).

Results

Morphology. Our morphological examination showed that the specimens of *Plestiodon* from the Balsas Basin

possess a postgenial scale bordered medially by a scale wider than long, a character state that supports their inclusion in the *P. brevirostris* group (Robinson 1979). Furthermore, the sample shares a set of traits that distinguish it from all the species currently assigned to the *P. brevirostris* group; the posterior contact between the parietals (enclosing the interparietal posteriorly) and unique coloration being the more evident (Table 1). This suggests the Balsas Basin sample represents an independent evolutionary lineage within the *P. brevirostris* group.

Phylogenetics. The final alignments of the sequenced mitochondrial fragment, *MKL1*, and *R35* included 1330 bp, 891 bp, and 645 bp, respectively. Aligned mtDNA sequences for pairs MZFC-HE 30624 and 30626 and MZFC-HE 25385–25386 were identical and we removed one from each pair for the maximum likelihood analysis. The partition scheme for the likelihood analysis of the mtDNA proposed by PartitionFinder 2.1.1 and calculated using RAxML 8.0 (Stamatakis 2006) included three partitions: one including *16S*, *tRNA*s, and the first codon position of *ND1* and one each for the second and third codon positions of *ND1*. The partitions and substitution models used for the Bayesian analysis of the mtDNA were: one partition for the *tRNA-Leu* gene with the K80+G model; one for *16S*, the remaining *tRNA*s, and the first codon position of *ND1* with the HKY+I+G model; one for the second codon position of *ND1* with the GTR+I+G model; and one for the third codon position of *ND1* with the TN93+I+G model. For the species tree inference, *MKL1* was partitioned by codon position and the scheme for *R35* included one partition for the first and second codon positions and another one for the third. The *BEAST runs using the complex substitution models proposed by PartitionFinder 2.1.1 and relaxed molecular clock priors showed deficient sampling and did not converge. Thus, we assigned the HKY+G model and strict clock prior to all the partitions used in the inference of the species tree.

The phylogenetic position of *Plestiodon parviauriculatus*, *P. parvulus*, the individual samples of *P. dugesii* (which was not monophyletic), and a clade containing *P. lynxe* and *P. sumichrasti* differed between the mitochondrial trees inferred using maximum likelihood and Bayesian inference. However, when the poorly supported relationships in each tree were collapsed into polytomies the resulting topologies were highly congruent, only differing in the position of the individual haplotypes within *P. copei*. Thus, the two trees were summarized by adding the posterior probabilities to the maximum likelihood tree, collapsing the nodes that showed poor support values in both trees (Fig. 2). The phylogenetic relationships recovered in the summarized tree are similar to those obtained with mtDNA sequences in previous studies (Feria-Ortiz *et al*. 2011; Brandley *et al*. 2012), which only differ in the placement of the samples of *P. dugesii* and by showing the position of *P. parviauriculatus* as resolved (with low support, however). In our analyses, the haplotypes from the Balsas Basin formed a strongly supported clade (BS = 84, PP = 1) nested within the *P. brevirostris* group. The Balsas Basin clade was the sister taxon to *P. ochoterenae*, and this relationship was significantly supported (BS = 100, PP = 1). The clade conformed by the Balsas Basin clade and *P. ochoterenae* appears as sister to a clade containing the haplotypes of *P. bilineatus*, *P. copei*, *P. dugesii*, and *Plestiodon* sp. Colima-Jalisco, although with a non-significant BS (BS = 64, PP = 0.99). Within the Balsas Basin clade, a haplotype from Arcelia, Guerrero, appears as sister to a strongly supported clade (BS = 97, PP = 0.97) containing the remaining samples from the Balsas Basin and is connected to them by a relatively long branch. The mean p-distance for the mtDNA alignment between the clade from the Balsas Basin and *P. ochoterenae*, as well as between the sample from Arcelia and *P. ochoterenae*, is 0.07; between the sample from Arcelia and the remaining haplotypes in the Balsas Basin 0.04, within the Balsas Basin clade 0.02, within the Balsas Basin clade without the sample from Arcelia 0.01, and within *P. ochoterenae* 0.003.

The species tree obtained in *BEAST shows low support values in general (Fig. 3). Support for the monophyly of the *Plestiodon brevirostris* group is high (PP = 1). In accordance with the mtDNA tree, *P. dugesii* is not monophyletic. The following clades were strongly supported: *P. bilineatus* + *P. dugesii* + *Plestiodon* sp. Colima-Jalisco (PP = 1); *P. brevirostris* + *P. indubitus* (PP = 0.98); and *P. lynxe lynxe* + *P. sumichrasti* (PP = 0.97). The first two clades were strongly supported in multi-locus trees presented in previous studies (Brandley *et al*. 2012; Bryson *et al*. 2017). The sample from Arcelia and the remaining samples from the Balsas Basin form a strongly supported clade (PP = 0.97) and they appear as sister to *P. ochoterenae* with a relatively high but non-significant support value (PP = 0.87). Same as in the mtDNA tree, the clade containing the samples from the Balsas Basin and *P. ochoterenae* appears as sister to a clade containing *P. bilineatus*, *P. copei*, *P. dugesii*, and *Plestiodon* sp. Colima-Jalisco, but with a non-significant support value (PP = 0.77).

Species delimitation. All our non-randomized analysis supported the recognition of three species within the clade containing the Balsas Basin samples and *P. ochoterenae*. The PPs for the three-species model and for each of the delimited species was high for each set of ancestral size and divergence time priors (PP = 1, in every case). *Plestiodon ochoterenae*, the sample from Arcelia, and the clade containing the remaining samples from the Balsas

Basin were each supported as a distinct species (Fig. 3). The results of the randomized analyses were as expected, granting confidence to the results of the non-randomized analyses. When the sequences were shuffled between all the species, the model with the highest PP recognized only one species. When the sequences were shuffled between the sample of Arcelia and the remaining samples from the Balsas Basin, the model with the highest PP recognized two species: *P. ochoterenae* plus a single species for the Balsas Basin.

EVS. We calculated the EVS of the new species at 16 (score for the first, second, and third scales = 5, 7, and 4, respectively), falling within the high vulnerability category (Wilson *et al*. 2013). Wilson *et al*. (2013) assigned a score of three in the third scale to all the species of *Plestiodon* distributed in Mexico. However, we consider that a score of four is more appropriate, given that lizards of the genus are believed to be venomous and deliberately killed in most towns we have visited.

Summary. Our morphological examination showed that the sample from the Balsas Basin is assignable to the *Plestiodon brevirostris* group and distinguishable from the closely related *P. ochoterenae* and the other species in the group (see below). Furthermore, the Balsas Basin and *P. ochoterenae* clades are concordant with geography, mutually exclusive, and moderately divergent from each other. BP&P 3.3 proposed to split the Balsas Basin clade in two species, one for the specimen from Arcelia and one for the remaining samples. However, sampling between Arcelia and the collecting sites of the other specimens is deficient and they are indistinguishable morphologically (see below) and clearly closely related. Additionally, it is generally accepted that over-splitting taxa is harmful for taxonomy and conservation (Carstens *et al*. 2013). Thus, we consider the sample from Arcelia as cospecific with the remaining samples from the Balsas Basin at present. Based on these results, we consider the whole sample of *Plestiodon* from the Balsas Basin as a new species, which we name and describe below.

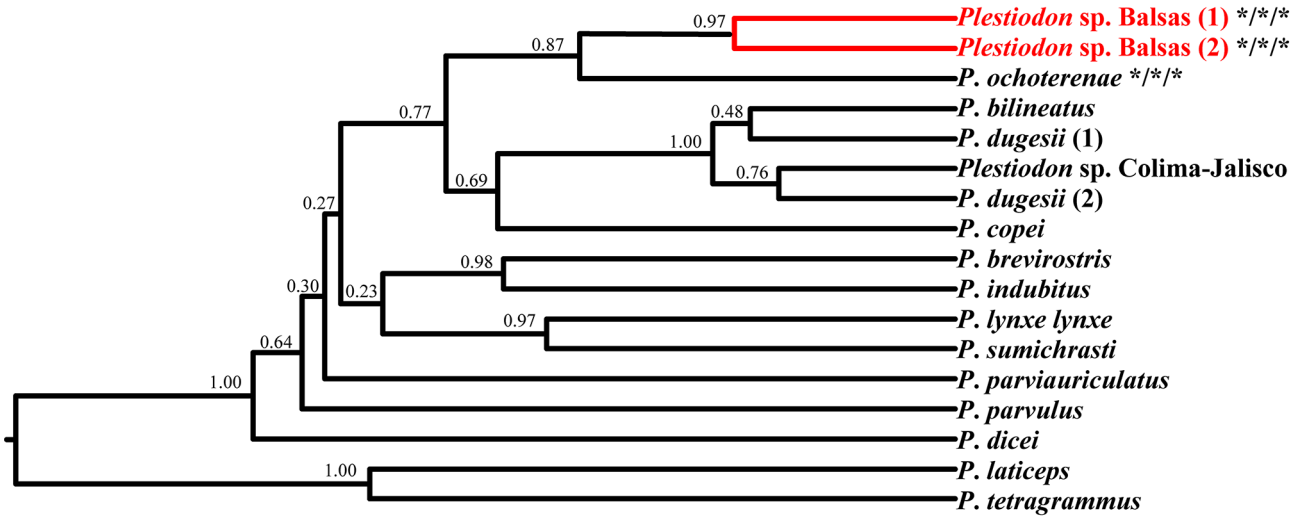

FIGURE 3. Species tree based on one mitochondrial and two nuclear loci. *Plestiodon* sp. Balsas (1) stands for a sample from Arcelia, Guerrero, and *Plestiodon* sp. Balsas (2) for the clade containing the remaining samples from the Balsas Basin. *Plestiodon dugesii* (1) and (2) stand for the samples with reference numbers 32 and 35, respectively. Numbers above branches indicate PPs. Asterisks next to terminals in the *P. ochoterenae* + *Plestiodon* sp. Balsas clade indicate PP $\geq$ 0.95 for the probability that each represents a distinct species as proposed by BP&P 3.3 under each of the three used combinations of priors for root age and ancestral population size used (see text).

Species account

Plestiodon lotus sp. nov.

(Figs. 4, 5)

Plestiodon brevirostris brevirostris (Günther, 1860) (in part); Feria-Ortiz *et al*. (2011:40–41, 43–47, 50, Table 6)
Plestiodon brevirostris (Günther, 1860) (in part); Feria-Ortiz *et al*. (2011:46)
Plestiodon indubitus (Taylor, 1933) (in part); Feria-Ortiz & García-Vázquez (2012:57–58, 63–64, 66, 68, Table 1)

Holotype. MZFC-HE 30621. Adult male. 5.6 km N Xixila, Municipality of Olinalá, Guerrero, Mexico, 17°59'42" N, 98°50'32" W (datum = WGS84), 1525 m elevation. Collected by Víctor H. Jiménez-Arcos on 30 October 2011.

Paratypes. Thirteen specimens. GUERRERO: Municipality of Arcelia: Cañada El Limón, Campo Morado, 18°11'40" N, 100°10'2" W, 1173 m elevation (MZFC-HE 19787); Municipality of Atlixtac: 0.2 km from Petatlán graveyard (CNAR 24264); 0.3 km from Petatlán graveyard (CNAR 24265); Municipality of Leonardo Bravo: 3 km N La Escalera (CNAR 6585); Municipality of Olinalá: 2.7 km N Xixila, 17°58'1" N, 98°50'38" W, 1545 m elevation (MZFC-HE 30620); 5.3–5.4 km N Xixila, 17°59'36" N, 98°51'2" W, 1490 m elevation (MZFC-HE 30624), 17°59'36" N, 98°51'3" W, 1493 m elevation (MZFC-HE 30625), 17°59'34" N, 98°51'4" W, 1535 m elevation (MZFC-HE 30626). MORELOS: Municipality of Temixco: Acatlipa (CNAR 1774); Municipality of Tepalcingo: Sierra de Huautla, near Estación El Limón, 18°33'26" N, 98°56'43" W, 1420 m elevation (MZFC-HE 30622). OAXACA: Municipality of Santiago Tamazola: La Casita, Santiago Tamazola, 17°41'39" N, 98°14'39" W, 1770 m elevation (MZFC-HE 17503); Municipality of Silacayoápam: 5 km NE Santiago Tamazola, 17°42'46" N, 98°12'22" W, 1629 m elevation (MZFC-HE 30623). PUEBLA: Municipality of Chiautla: 11 km ESE Chiautla de Tapia, dirt road to San Juan de los Ríos, 18°14'15" N, 98°29'32" W, 1074 m elevation (MZFC-HE 30627).

Diagnosis. *Plestiodon lotus* can be distinguished from the other members of the *P. brevirostris* group as follows: from *P. bilineatus* and *P. dicei*, by the presence of a primary temporal (versus primary temporal absent in 89.4% [n = 52] of *P. bilineatus* and 98% [n = 52] of *P. dicei*); additionally from *P. bilineatus* by having a tendency towards more Toe-IV lamellae (13–15 [$\bar{X}$ = 13.81, n = 27], versus 11–13 [$\bar{X}$ = 11.7, n = 54] in *P. bilineatus*); and from *P. dicei* by having the interparietal enclosed posteriorly by the parietals (versus interparietal not enclosed posteriorly by the parietals in 94.2% [n = 52] of specimens in *P. dicei*).

Plestiodon lotus differs from *P. brevirostris*, *P. copei*, *P. nietoi*, *P. ochoterenae*, and *P. parviauriculatus* by having the primary lateral dark lines separated medially by the six median dorsal scale rows and upper half of the adjacent row on each side at the level of midbody (versus primary lateral dark lines separated medially by the median six dorsal scale rows or less invariably in the other species, except for 9.01% of the specimens [n = 122] of *P. brevirostris*); additionally from *P. brevirostris*, *P. copei*, *P. ochoterenae*, and *P. parviauriculatus* by having the interparietal enclosed posteriorly by the parietals (versus interparietal not enclosed posteriorly by the parietals in 82.64% [n = 122] of *P. brevirostris*, 96.77% [n = 62] of *P. copei*, 85.71% [n = 7] of *P. ochoterenae*, and 97% [n = 27] of *P. parviauriculatus*); and from *P. brevirostris*, *P. copei*, and *P. nietoi* by having a faint lower secondary dark line at the level of the neck (versus lower secondary dark line conspicuous at the level of the neck in the other species).

Plestiodon lotus differs from *P. colimensis* by having limbs that do not overlap when adpressed against the body (versus limbs overlapping when adpressed against the body in *P. colimensis*), a tendency towards fewer longitudinal dorsal scale rows around midbody (23–26 [$\bar{X}$ = 24.43, n = 14], versus 26–28 [$\bar{X}$ = 27, n = 4] in *P. colimensis*), and a tendency towards fewer Toe-IV lamellae (13–15 [$\bar{X}$ = 13.81, n = 27], versus 13–17 [$\bar{X}$ = 15.38, n = 8] in *P. colimensis*); from *P. dugesii* by having four supraoculars (versus three in *P. dugesii*); from *P. indubitus* and *Plestiodon* sp. Colima-Jalisco by having a solid lateral light line at level of neck (versus lateral light line replaced by a series of scales with white anterior edges and centers and black posterior borders in 90.91% [n = 33] of *P. indubitus* and 100% [n = 35] of *Plestiodon* sp. Colima-Jalisco); additionally from *P. indubitus* by having the light coloration of the supralabials extending to the lip border (versus light coloration separated from lip border on the sixth and seventh supralabials); from *P. lynxe belli, P. l. lynxe* and *P. sumichrasti* by having the interparietal enclosed posteriorly by the parietals (versus interparietal not enclosed posteriorly by the parietals in 100% [n = 36] of *P. l. belli*, 94.74% [n = 92] of *P. l. lynxe*, and 85.71% [n = 21] of *P. sumichrasti*) and lacking a light median line in all growth stages (versus dorsum bearing a light median line that is conspicuous in juveniles and faint in large adults); and from *P. parvulus* by having a relatively long dorsolateral light line extending posteriorly to the anterior fourth of the body or beyond (versus dorsolateral light line extending barely posteriorly past the shoulder in *P. parvulus*).

Description of holotype (Fig. 4). Adult male with both hemipenes partially everted. Snout–vent length (SVL) 53.1 mm; distance between tip of snout and anterior margin of orbit 4.6 mm, between tip of snout and anterior insertion of fore-limb 17.8 mm; trunk length 27.4 mm; head width 8.3 mm; head length 11.0 mm; tail complete, 64.1 mm in length. Limbs moderate in length, fingertips of fore-limb and hind limb separated from each other when limbs adpressed against body; straightened fore-limb (from base to tip of longest finger) 14.9 mm (28% SVL), straightened hind limb (from base to tip of longest toe) 15.6 mm (29.3% SVL); outer posterior tubercles of wrist and palm enlarged.

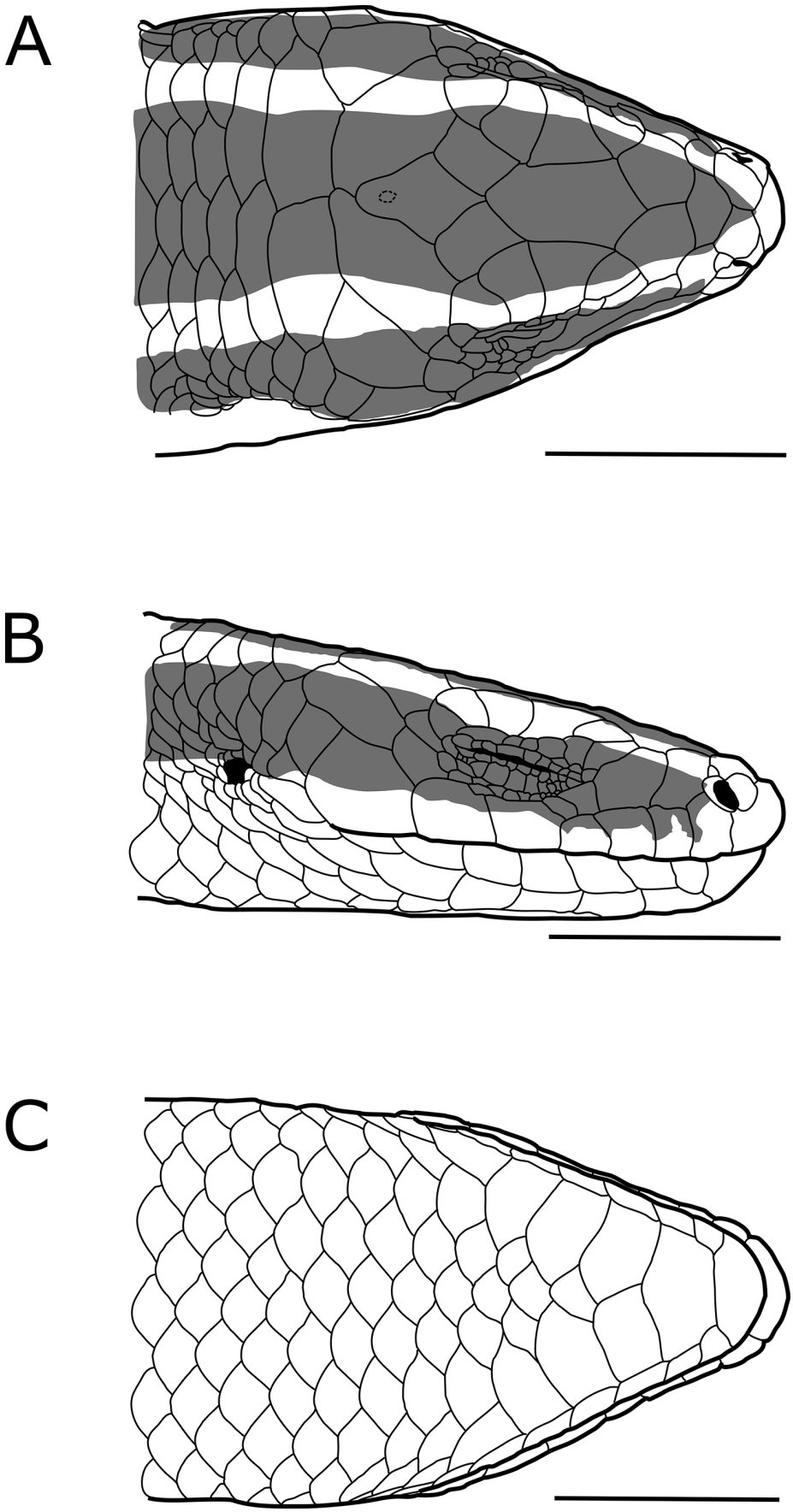

FIGURE 4. *Plestiodon lotus*, head of holotype (MZFC-HE 30621) in (A) dorsal, (B) right lateral, and (C) ventral views. Scale bars = 5 mm.

Snout rounded in dorsal and lateral view. Rostral 1.8 × wider than high, in broad contact with supranasals posteriorly; supranasals 1.2 × wider than long, in broad contact with each other and each with nasal, right supranasal with short oblique suture separating its posterolateral corner from rest of scale; frontonasal 1.8 × wider than long, posterior margin v-shaped, in contact with prefrontals posteriorly; prefrontals in contact with each other medially, 1.1/1 × wider than long, posterior margins v-shaped, in contact with first supraocular, anterior and posterior loreals, and first superciliary; frontal large, elongate, hexagonal, 1.9 mm wide, 3.2 mm long; in broad contact with prefrontals; in narrow contact with first and third supraoculars and wide contact with second supraocular on left side, in broad contact with second supraocular and narrow contact with third supraocular on right side; and in broad and narrow contact with frontoparietals and interparietal, respectively; frontoparietals narrowly separated from each other medially, in contact with third and fourth supraoculars laterally, and parietals and interparietal posteriorly; supraoculars four; first supraocular smaller than second and third, in lateral contact with first and second superciliaries; second supraocular largest, in lateral contact with second, third, fourth, and fifth superciliaries; third supraocular in lateral contact with fifth and sixth superciliaries; fourth supraocular smaller than second and third, in contact with sixth and seven superciliaries laterally and parietal posteriorly; interparietal small (2 mm wide, 2.7 mm long), slightly elongate, kite-shaped, in contact with parietals laterally and posteriorly; pineal foramen barely visible; parietals large, elongate, obliquely oriented, in medial contact with each other posteriorly, in contact with last superciliary, upper postsubocular, and upper secondary temporal laterally on each side, and in contact with left anterior nuchal on left side and both anterior nuchals on right side posteriorly; two pairs of large nuchals, scales of each pair in medial contact with each other; anterior nuchals 2.3/2.2 × wider than long; posterior nuchals 4.3 × wider than long; anterior nuchals in contact with parietals, upper secondary temporal and upper tertiary temporal.

Nasal divided in anterior and posterior halves, in contact with rostral; loreals 2/2; anterior loreal 1.7/1.2 × higher than long, divided horizontally on left side, in contact with first and second supralabials, posterior nasal, and posterior loreal; posterior loreal 1.3/1.4 × longer than high, notably larger than anterior loreal, in contact with anterior presubocular and second and third supralabials; preoculars 1/1, small; presuboculars 2/2, anterior presubocular in contact with third and fourth supralabials, posterior presubocular in contact with fourth and fifth supralabials; superciliaries 7/7; first superciliary largest, in contact with preocular ventrally; second to fifth superciliaries gradually becoming shorter and lower posteriorly; sixth superciliary nearly as high as fifth, horizontally elongate; last superciliary higher than anterior ones except first; upper palpebrals 9/10; lower palpebrals 10/11; lower eyelid movable; no transparent window in lower eyelid; 5/5 enlarged rectangular scales on lower eyelid; postoculars 2/2, small; postsuboculars 3/4; first postsubocular in contact with fifth and sixth supralabials, second postsubocular in contact with sixth supralabial and primary temporal, third postsubocular in contact with primary temporal and upper secondary temporal on left side, in contact with primary temporal on right side; fourth postsubocular on right side in contact with primary temporal and upper secondary temporal; temporal formula 1 + 2 + 1; primary temporal in contact with upper secondary temporal and sixth and seventh supralabials; upper secondary temporal large, in contact with tertiary temporal, lower secondary temporal, and sixth supralabial; lower secondary temporal vertically elongate, approximately as large as primary temporal, smaller than upper secondary temporal, separated from primary temporal by contact between upper secondary temporal and seventh supralabial; tertiary temporal large, 1.8/2.6 × higher than long; supralabials 7/7, first four gradually becoming lower posteriorly; fifth and sixth similar in size, larger than first four; seventh largest; postlabials 2/2.

Mental 2.5 × wider than long; infralabials 7/7; postmental larger than mental, in contact with anteriormost three and two infralabials on left and right side, respectively; three pairs of enlarged chinshields; first pair in broad contact with each other medially, second pair separated by one midgular scale, third pair separated by three midgular scales; scale bordering postgenial medially wider than long.

External ear opening rounded, smaller than eye opening, without lobules or spines; body scales smooth or barely striated, arranged in 28 longitudinal rows around neck just anterior to forearm, in 24 rows around midbody, in 13 rows around base of tail; dorsals in 51 transverse rows from nuchals to level above vent, subequal in size to ventrals; scales of limbs smooth or barely striated as in body; digits short; supradigital scales in one row; subdigital lamellae counts (following Myers and Donnelly, 1991): hand: I 5/6 II 8/8 III 9/9 IV 10/10 V 6/7; foot: I 5/5 II 8/8 III 11/11 IV 13/13 V 9/9.

Median enlarged preanal scales nearly twice as wide as adjacent ventrals; first two transverse subcaudal rows as large as ventrals, remaining subcaudals about twice as wide.

Color in preservative (holotype). Middorsal light area olive (Greenish Olive 125); bordered on each side by dorsolateral light line (latter lines fusing with each other anteriorly on rostral and supranasals). Dorsolateral light lines light gray (Dark Pearl Gray 290), occupying lower half of second and upper half of third dorsal scale rows at level of midneck; occupying lower half of second, third, and upper half of fourth dorsal scale rows at midbody; gradually fading posteriorly to hind limbs. Upper secondary dark line dark brown (Sepia 279), bordering dorsolateral light line medially; solid, continuous on neck and anterior fourth of body; replaced by series of dark speckles on head, posterior three-fourths of body, and anterior half of tail; occupying upper half of second dorsal scale row at level of midneck; occupying middle portion of second dorsal scale row at level of midbody. Primary lateral dark line light brown on head (Dark Brownish Olive 127), darkening posteriorly (Sepia 279); beginning anteriorly on posterior nasal and ending posteriorly at level of hind limbs; bordering dorsolateral light line laterally; occupying lower half of third, fourth and fifth, and upper half of sixth dorsal scale rows at level of midneck; occupying lower half of fourth, fifth, and upper half of sixth dorsal scale rows at level of midbody. Lateral light line bluish gray (Pratt's Payne's Gray 293), bordering primary lateral dark line ventrally, partially fused at level of neck with light ventral coloration, but clearly comprising lower half of sixth and nearly all of seventh scale row; becoming indistinguishable from light ventral coloration at level of anterior insertion of fore-limb. Light ventral coloration light cream (Light Buff 2); fusing with dorsolateral light line on rostral and nasal; extending dorsally to mid supralabials (i.e., no discernible lateral light line on supralabials) at level of head, bordering lateral light line and primary lateral dark line ventrally at levels of neck and body, respectively; lateral borders throughout body and medial surface of posterior three-fourths of body heavily suffused with bluish gray (Pratt's Payne's Gray 293). Dorsal surface of limbs olive (Greenish Olive 125); ventral surface of fore-limbs and hind limbs light cream (Light Buff 2) and bluish gray (Pratt's Payne's Gray 293), respectively. Dorsal and lateral surfaces of anterior half of tail olive (Greenish Olive 125) and bluish gray (Pratt's Payne's Gray 293), respectively; dorsal and lateral surfaces of posterior half of tail dark gray (Medium Plumbeous 294); ventral surface of tail light cream (Light Buff 2).

Color in life (Fig. 5). The present section is based on photographs of the paratypes in life. Dorsal surface of head, mid-dorsal light area, and anterior portion of tail ranging from brownish silver to metallic gold, posterior border of each scale dark; dorsolateral light line broad, faint, yellowish cream, somewhat diffuse in large specimens; narrower, conspicuous, clear-cut in small ones; primary lateral dark line dark brown; lower portion of supralabials yellowish cream, suffused with orange in males; lateral light line light gray; infralabials and gular region yellowish cream, suffused with orange in males; ventral surface of body light gray with suffusion of light blue; ventral surface of anterior portion of tail light gray with suffusion of orange; posterior portion of non-regenerated tail electric blue.

Variation (measurements in mm). Noteworthy variation in the type series (n = 14, including holotype) is described below. The holotype is included to ease comparison with other species. The diagnostic traits of *Plestiodon lotus* were observable in specimen CNAR 1774, but considerable damage to the specimen prevented the recording of the number of supraoculars contacting the frontal, postsuboculars, postsuboculars contacting the sixth supralabial, and the presence or absence of contact between the upper postsubocular and the upper secondary temporal. Thus, CNAR 1774 is excluded from the reported variation in those traits. Additionally, the following characters could only be recorded on the left side: number of superciliaries, scales contacting the upper secondary temporal between the upper postsubocular and the first nuchal, postlabials, and the scales contacting both the upper secondary temporal and the upper postlabial.

Frontonasal absent in one specimen (CNAR 24264); frontonasal and frontal in contact in four specimens (CNAR 24265; MZFC-HE 24159, 30623–30624); supraoculars contacting frontal 2–3, $\bar{X}$ = 2.88 (2/2 one; 3/2 one; 3/3 eleven, including holotype); postnasals present in one specimen (MZFC-HE 30622); anterior loreal divided horizontally on left side in one specimen (MZFC-HE 30621, holotype); contact between upper presubocular and third supralabial present on both sides in eleven specimens (including holotype), on left and right side in one specimen each, absent on both sides in one; superciliaries 6–8, $\bar{X}$ = 7 (6/7 one; 7/7 eleven, including holotype; 7/8 one; 7 on left side of CNAR 1774); postsuboculars 3–5, $\bar{X}$ = 3.77 (3/3 two; 3/4 one [holotype]; 4/3 two; 4/4 seven; 4/5 one); postsuboculars contacting sixth supralabial 2–3, $\bar{X}$ = 2.42 (2/2 seven, including holotype; 3/2 one; 3/3 five); primary temporal in dorsal contact with parietal, separating upper postsubocular from upper secondary temporal, on right side in one specimen (MZFC-HE 17503); sixth supralabial divided horizontally in one specimen (MZFC-HE 30622); scales contacting upper secondary temporal between upper postsubocular and first nuchal 3–5, $\bar{X}$ = 3.78 (3/3 three; 4/3 one; 4/4 eight, including holotype; 4 on left side of CNAR 1774; 5/4 one); seventh

supralabial contacting upper secondary temporal in eight specimens (CNAR 24265; MZFC-HE 19787, 30620–30621, 30623, 30625–30627), separated from each other by an extended lower secondary temporal in six (CNAR 1774, 6585, 24264; MZFC-HE 24159, 30622, 30624); postlabials 1–3, $\bar{X}$ = 1.89 (1/1 one; 1/2 one; 2/1 one; 2/2 nine, including holotype; 2/3 one; 2 on left side of CNAR 1774); scales as large as, or larger than, upper postlabial contacting it 2–5, $\bar{X}$ = 3.89 (2/4 one; 3/4 one; 4/2 one; 4/3 one; 4/4 seven, including holotype; 4 on left side of CNAR 1774; 5/4 one; 5/5 one); scales contacting both upper secondary temporal and upper postlabial 1–3, $\bar{X}$ = 2.41 (1/2 two; 2/1 one; 2/2 two; 2/3 one; 2 on left side of CNAR 1774; 3/2 one; 3/3 six, including holotype).

Transverse dorsal scale rows between nuchals and level above vent 51–57, $\bar{X}$ = 53.07 (51 four; 52 one [holotype]; 53, four; 54, two; 55, two; 57, one); longitudinal dorsal scale rows around midbody 23–26, $\bar{X}$ = 24.43 (23 two; 24 eight, including holotype; 26 four); Toe-IV lamellae 13–15, $\bar{X}$ = 13.81 (13/13 three, including holotype; 13/14 one, 14/14 eight;14 on right side, non-recordable on left side, in MZFC-HE 19787; 15/15 one;).

SVL 28.68–65.58, $\bar{X}$ = 51.04; SVL / trunk length ratio 1.65–1.96, $\bar{X}$ = 1.83; SVL / head length ratio 4.52–5.7, $\bar{X}$ = 5.08; SVL / tibia length ratio 8.81–11.94, $\bar{X}$ = 9.66.

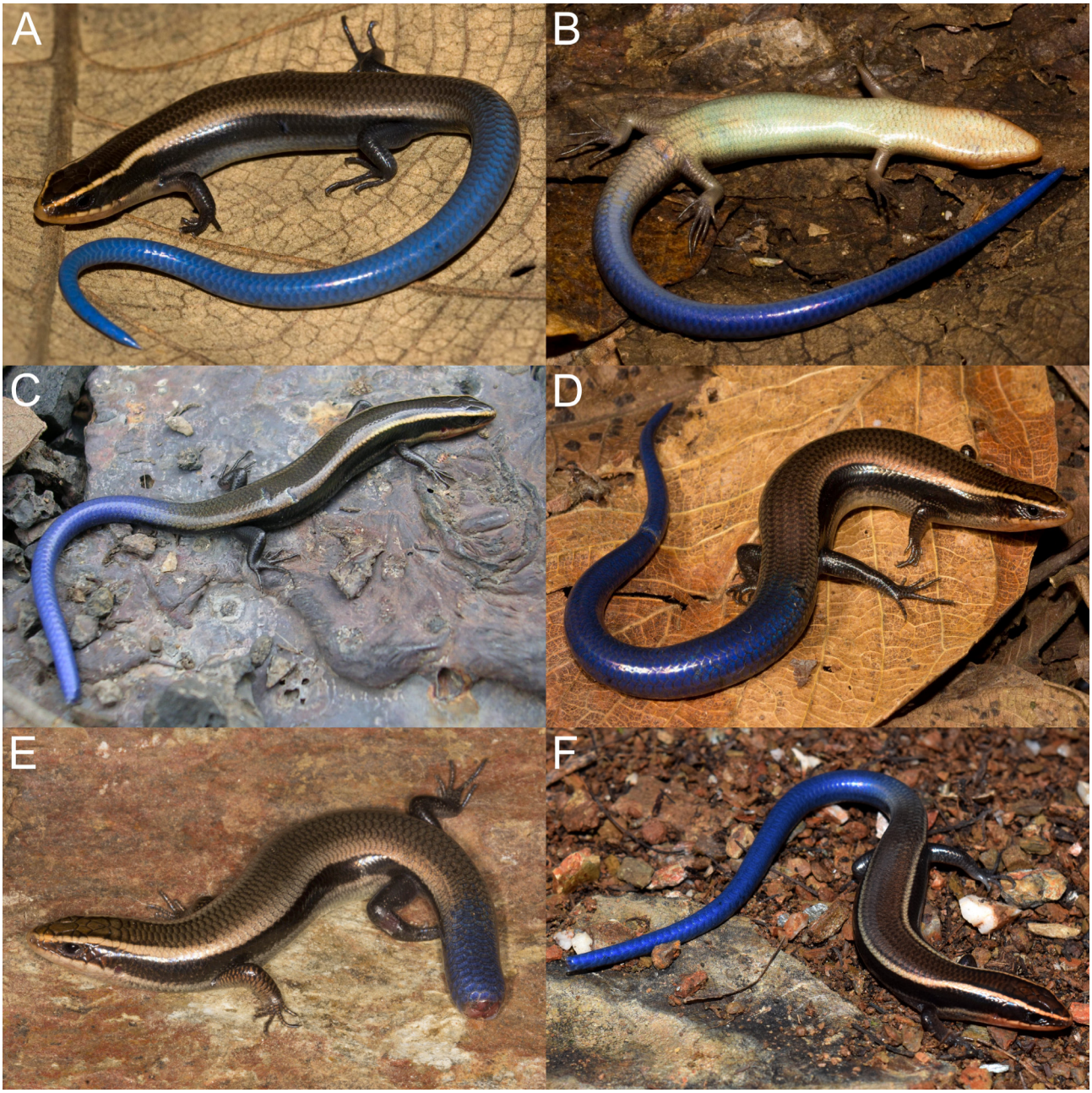

FIGURE 5. Paratypes of *Plestiodon lotus* in life. Specimens from: (A, B) the vicinities of the type locality, Olinalá, Guerrero (MZFC-HE 30624 and 30625, respectively); (C) Arcelia, Guerrero (MZFC-HE 19787); (D) Tepalcingo, Morelos (MZFC-HE 30622); (E) Silacayoápam, Oaxaca (MZFC-HE 30623); and (F) Chiautla, Puebla (MZFC-HE 30627).

This paragraph is based on specimens preserved in ethanol and some lines are likely less discernible than in life. Upper secondary dark line extending posteriorly to posterior end of neck in one specimen (CNAR 6585), to forearms in nine (CNAR 1774; MZFC-HE 17503, 19787, 30621–30626), and to posterior end of anterior fourth of body in four (CNAR 24264–24265; MZFC-HE 30620, 30627); dorsolateral light line extending posteriorly to posterior end of anterior fourth of body in four specimens (MZFC-HE 30621, 30623–30625), to midbody in one (MZFC-HE 30622), to hind limbs in one (CNAR 24265), and to anterior portion of tail in eight (CNAR 1774, 6585, 24264; MZFC-HE 17503, 19787, 30620, 30626–30627); lateral light line extending dorsally to sixth scale row at level of mid-neck in 10 specimens (CNAR 1774, 6585, 24264–24265; MZFC-HE 19787, 30621–30622, 30624–30626), and to seventh scale row in four (MZFC-HE 17503, 30620, 30623, 30627).

Remarks. The sample of *Plestiodon lotus* from near Arcelia, Guerrero (MZFC-HE 19787) is molecularly divergent from the other samples assigned to the species (see above). However, the specimen from Arcelia is not morphologically distinguishable from the other specimens assigned to *P. lotus*. Furthermore, MZFC-HE 19787 represents the farthest record (ca. 140 km WNW in straight line) from the type locality of *P. lotus*, which may explain its genetic divergence from other samples. We were not able to obtain molecular data for specimen CNAR 6585, which is geographically intermediate between the specimen from Arcelia and the other sequenced samples of *P. lotus*. Additionally, photographic records suggest *P. lotus* is widespread in the Balsas Basin (see below). Thus, it seems likely that the apparent divergence between the sample from Arcelia and the remaining samples of *P. lotus* is an effect of deficient sampling in areas where *P. lotus* is expected to occur. Therefore, we provisionally assign the specimen from Arcelia to *P. lotus*.

Specimens from Morelos assigned to *Plestiodon brevirostris brevirostris* or regarded as putative intergrades between *P. b. brevirostris* and *P. b. indubitus* by Dixon (1969) might represent *P. lotus* (see Discussion). Unfortunately, those specimens could not be examined.

Etymology. The specific Latin name is treated as a participle in the nominative singular and means bathed, clean, elegant. It makes reference to the appearance of the new species, characterized by having fainter lines than its geographically closest congeners.

Distribution and ecology. *Plestiodon lotus* is known from 1074–1770 m elevation in the Balsas Basin of the Mexican states of Guerrero, Morelos, Oaxaca, and Puebla. It appears to be widespread in the area and photographic records suggest it may also be present in the vicinities of Amatlán de Quetzalcóatl, northern Morelos, and the Sierra de Nanchititla, western México state.

The specimens of the new species were found in oak and tropical deciduous forests (Fig. 6). Most of them were found under rocks or fallen logs, while some were active on the leaf litter. *Plestiodon lotus* appears to be more abundant in rocky hillsides with high tree density. Monthly surveys were conducted at the type locality and vicinities, where lizards were only seen between June and February. This suggests a reduction in activity in the warmer months (March to May) associated with the dry season. Vegetation at the type locality is oak forest, where *Quercus glaucoides*, *Q. castanae*, and *Q. magnoliifolia* dominate the arboreal stratum. Climatic variables extracted from BioClim (Hijmans *et al*. 2005) are as follows: mean annual temperature is 22.7°C, mean temperatures of the warmest and coldest quarter are 25.2°C and 20.1°C, respectively, and the mean annual precipitation is 885 mm.

There is no direct evidence that *Plestiodon lotus* is sympatric with other species of the genus. Seven other species of *Plestiodon* are found in Guerrero, Morelos, Oaxaca, and Puebla, but they differ from *P. lotus* in elevational range and/or are distributed in different biogeographic provinces (Fig. 7). *Plestiodon brevirostris* is found in mesic forest and xeric scrub at higher elevations of the Sierra Madre del Sur, the Transmexican Volcanic Belt, and the biogeographically complex intersection of this Belt with the Sierra Madre Oriental; *P. copei* and *P. indubitus* inhabit mesic forests at higher elevations of the Transmexican Volcanic Belt, though *P. indubitus* is found fairly low in the Sierra de Taxco and the vicinities of Tepoztlán and Cuernavaca, where it probably comes into contact with *P. lotus*; *P. lynxe lynxe* inhabits a variety of habitats at usually higher elevations of the Central Mexican Plateau, Sierra Madre Occidental, Sierra Madre Oriental, and Transmexican Volcanic Belt; *P. nietoi* is found in mesic forest at higher elevations of the Sierra Madre del Sur; *P. ochoterenae* inhabits similar elevations to *P. lotus* in the Sierra Madre del Sur and both species probably come into contact in the continental slopes of the aforementioned sierra (e.g., near Chilapa de Álvarez, Guerrero); and *P. sumichrasti* is found in tropical forest at lower elevations of the Veracruzan province (Feria Ortiz 2011; Feria-Ortiz *et al*. 2011; Feria-Ortiz & García-Vázquez 2012; Lee 2000; Pavón-Vázquez, pers. obs.). The skink *Marisora brachypoda* (Taylor) is found in sympatry with *P. lotus* at the type locality and near Santiago Tamazola, Oaxaca—and presumably in other

localities—but differs in microhabitat preference favoring more open areas. *Mesoscincus altamirani* (Dugès) is another skink that might be sympatric with *P. lotus* in Guerrero (Mendoza Hernández *et al*. 2011; Jiménez-Arcos *et al*. 2016).

Discussion

The combination of traits in *Plestiodon lotus* might have contributed to the confusion regarding the alleged existence of gene flow between *P. brevirostris* and *P. indubitus*. Dixon (1969) noted that some specimens from between "Cuernavaca and Tepoztlán, Morelos" (between Tres Marías and Cuernavaca, according to Feria-Ortiz *et al*. 2011) had a combination of traits from the latter two species, namely "enclosed interparietals and a faint lateral light line on the neck or a non-enclosed interparietal without a lateral light line on the neck." The former combination of traits is characteristic of *P. lotus* and the species is expected to be distributed in the vicinities of Cuernavaca and Tepoztlán, as demonstrated by the specimen from Acatlipa and the photographic evidence from Amatlán de Quetzalcóatl. Acatlipa is located in the same alluvial fan as the gullies of Cuernavaca and both localities share the presence of tropical deciduous forest and oak forest (García Barrios *et al*. 2008). Other specimens of *P. brevirostris* from Morelos, for which Dixon (1969) provided no detailed description, might also represent *P. lotus* based on their distribution, namely specimens from Tepoztlán and the vicinities of Huajintlán.

Recurrent fieldwork in northern Morelos has proved *P. indubitus* to be abundant there but has failed to produce typical *P. brevirostris*. We were also unable to find typical *P. brevirostris* in the Sierra del Ajusco in the outskirts of Mexico City, another locality for which Dixon (1969) reported the species and in which it could come into contact with *P. indubitus*. Given our current understanding we consider that the presence of *P. brevirostris* and its hybridization with *P. indubitus* in Ciudad de México, western México state, and Morelos is unlikely. Thus, the presence of a non-enclosed interparietal and a well-defined lateral light line on the neck in specimens from the region is possibly due to intraspecific variation within *P. indubitus* and/or hybridization between this species and *P. copei*. The latter species typically exhibits both aforementioned traits and the existence of gene flow between both species is supported by preliminary analyses of microsatellite data (Alvarado-Avilés, unpublished data). Additional sampling of specimens and loci might help clarify the issue.

The present study highlights the importance of taking multiple lines of evidence into account when evaluating the species richness of a particular taxon or region. The discovery of new species worldwide, and in Mexico in particular, has been recently prompted by the use of both molecular and integrative approaches (e.g., Cruz-Barraza *et al*. 2012; Jadin *et al*. 2012; Bryson *et al*. 2014). While a number of alternate hypotheses regarding the taxonomic identity of *P. lotus* seemed possible based solely on morphology, the molecular data presented here helped to recognize it as a new species. This discovery further highlights the relevance of molecular data in elucidating species limits within the *P. brevirostris* group (e.g., Feria-Ortiz *et. al.* 2011; Brandley *et al*. 2012). It is notable that *P. lotus* is more easily distinguished from its sister species, *P. ochoterenae*, than from other species. Thus, the presence of either convergence, morphological conservatism (as suggested by Feria-Ortiz *et al*. 2011), or both within the *P. brevirostris* group seems likely and must be taken into consideration for future taxonomic work, as these phenomena can lead to the overlooking of cryptic diversity (Bond *et al*. 2001; Heideman *et al*. 2011; Moen *et al*. 2013).

The discovery of *Plestiodon lotus* from the Balsas Basin further supports the importance of the complex topography of central Mexico in promoting the diversification in several taxa (Bryson *et al*. 2004 and references therein) and the *P. brevirostris* group in particular (Brandley *et al*. 2012; Bryson *et al*. 2017). The Balsas Basin has been identified as the area with the highest potential richness of endemic reptiles in Mexico, resulting in part from the presence of suitable vegetation types (Ochoa Ochoa & Flores Villela 2006). Unfortunately, central Mexico is the region with the highest population density in the country (Ochoa Ochoa & Flores Villela 2006). Additionally, both oak and tropical deciduous forests have been severely affected by agriculture, grazing, touristic development, and more recently by open-pit mining in the Balsas Basin (Rzedowski 1983; Ceballos & García 1995; Mendoza-Hernández, pers. obs.). With regard to *Plestiodon lotus*, the oak forest at the collecting locality of the specimen from Arcelia was replaced by an open-pit mine. The vulnerability of the new species is evidenced by its high EVS. We invite the Mexican government, private institutions, and local landowners to start new conservation projects and continue those existent in order to protect *P. lotus* and the other species that inhabit the Balsas Basin.

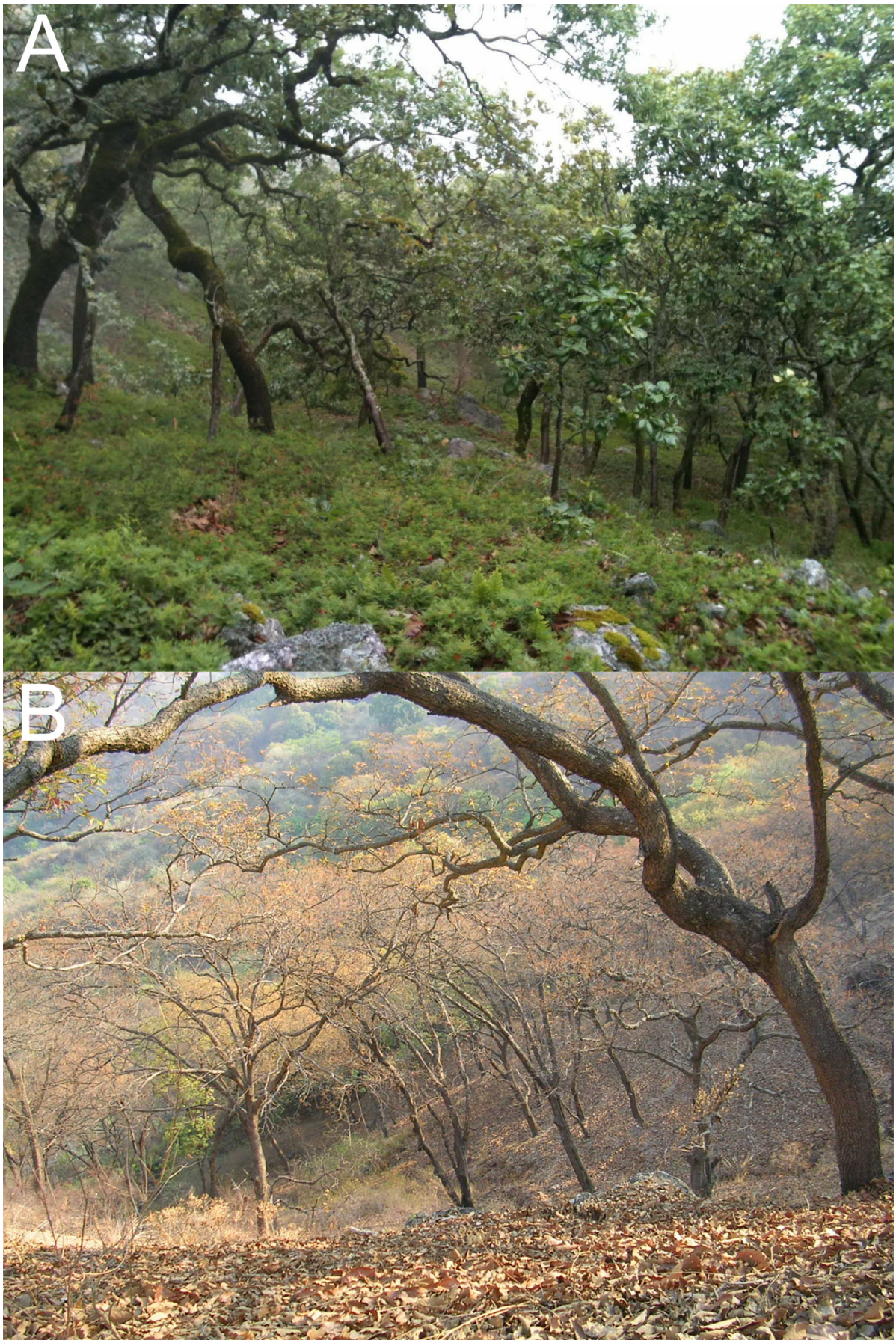

FIGURE 6. Habitat of *Plestiodon lotus* at (A) the type locality near Olinalá, and (B) Arcelia, both in Guerrero.

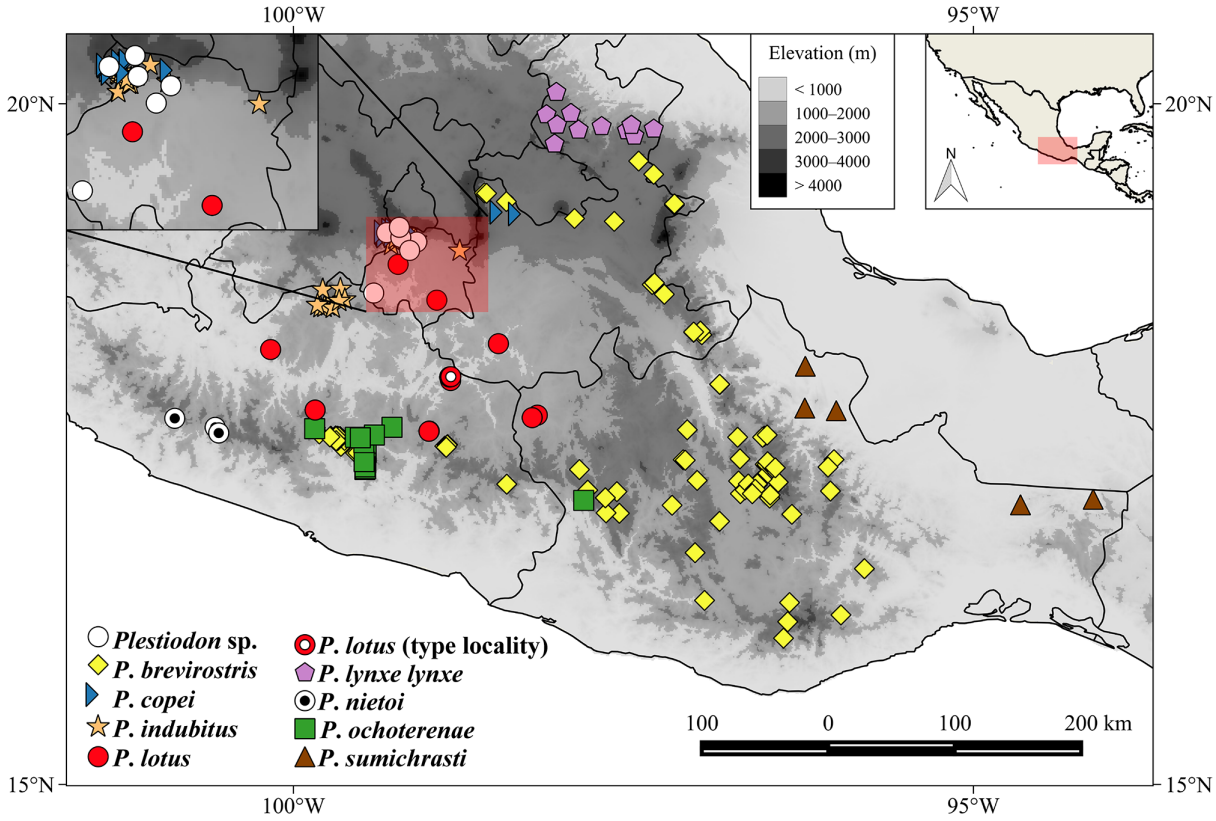

FIGURE 7. Collecting localities of the species of the *Plestiodon brevirostris* group in the Mexican states of Guerrero, Morelos, Oaxaca, and Puebla. The white circles represent likely records of *P. lotus*, *P. indubitus*, or hybrids between *P. indubitus* and *P. copei* (see text).

Acknowledgments

This paper is based upon work supported by a grant from CONACYT (no. 154093) to A. Nieto-Montes de Oca. We thank the Posgrado en Ciencias Biológicas and CONACYT for supporting the graduate education of V.H. Jiménez-Arcos and C.J. Pavón-Vázquez; J. Carlos Alvarado Avilés, Uri O. García Vázquez, and Giovany A. González Desales for sharing relevant data; Héctor Archundia Nieto for helping to draw Fig. 4; José C. Arenas Monroy, Juan Esteban Flores, Héctor C. Olguín Monroy, Octavio Rojas Soto, Enrique Rosendo Rodríguez, and Leopoldo Vázquez Reyes for their assistance in the field; Armando Borgonio Valencia, Adriana J.X. González Hernández, and Víctor H. Reynoso Rosales (CNAR), as well as Oscar Flores Villela, Leticia Ochoa Ochoa, and Edmundo Pérez Ramos (MZFC-HE) for granting access to herpetological collections; Emily Braker (UCM), Alan Resetar (FMNH), Gregory Schneider (UMMZ), Luke Welton (KU), and Aquila Wilks (FMNH) for sending photographs of relevant specimens; Ian G. Brennan, Cameron D. Siler, and an anonymous reviewer for providing insightful comments that substantially improved the quality of this work; Manuel E. Vargas Orrego for allowing us to use one of his photographs (Fig. 5F); Luis Canseco Márquez and Manuel E. Vargas Orrego for donating specimens; Fernando Jaramillo Monroy for sharing relevant literature; and Bernardo Rosendo Ponce for his logistical support. Fieldwork was covered by collecting permit SEMARNAT # FAUT-0093 issued to A. Nieto-Montes de Oca.

References

Bond, J.E., Hedin, H., Ramírez, M.G. & Opell, B.D. (2001) Deep molecular divergence in the absence of morphological and ecological change in the Californian coastal dune endemic trapdoor spider *Aptostichus simus*. *Molecular Ecology*, 10, 899–910.
https://doi.org/10.1046/j.1365-294x.2001.01233.x

Bouckaert, R., Heled, J., Kühnert, D., Vaughan, T., Wu, C.-H., Xie, D., Suchard, M.A., Rambaut, A. & Drummond, A.J. (2014) BEAST 2: A Software Platform for Bayesian Evolutionary Analysis. *PLoS Computational Biology*, 10, e1003537.

https://doi.org/10.1371/journal.pcbi.1003537
Brandley, M.C., Wang, Y., Guo, X., Nieto-Montes de Oca, A., Feria-Ortiz, M., Hikida, T. & Ota, H. (2011) Accommodating high rates of evolution in molecular divergence dating methods: an example using inter-continental dispersal of *Plestiodon* (*Eumeces*) lizards. *Systematic Biology*, 60, 3–15.
https://doi.org/10.1093/sysbio/syq045
Brandley, M.C., Ota, H., Hikida, T., Nieto-Montes de Oca, A., Feria-Ortiz, M., Guo, X. & Wang, Y. (2012) The phylogenetic systematics of blue-tailed skinks (*Plestiodon*) and the family Scincidae. *Zoological Journal of the Linnean Society*, 165, 163–189.
https://doi.org/10.1111/j.1096-3642.2011.00801.x
Bryson Jr., R.W., Linkem, C.W., Dorcas, M.E., Lathrop, A., Jones, J.M., Alvarado-Díaz, J., Grünwald, C.I. & Murphy, R.W. (2014) Multilocus species delimitation in the *Crotalus triseriatus* species group (Serpentes: Viperidae: Crotalinae), with the description of two new species. *Zootaxa*, 3826 (3), 475–496.
https://doi.org/10.11646/zootaxa.3826.3.3
Bryson Jr., R.W., Linkem, C.W., Pavón-Vázquez, C.J., Nieto-Montes de Oca, A., Klicka, J. & McCormack, J.E. (2017) A phylogenomic perspective on the biogeography of skinks in the *Plestiodon brevirostris* group inferred from target enrichment of ultraconserved elements. *Journal of Biogeography*, 44, 2033–2044.
https://doi.org/10.1111/jbi.12989
Carstens, B.C., Pelletier, T.A., Reid, N.M. & Satler, J.D. (2013) How to fail at species delimitation. *Molecular Ecology*, 22, 4369–4383.
https://doi.org/10.1111/mec.12413
Ceballos, G. & García, A. (1995) Conserving neotropical biodiversity: the role of dry forests in western Mexico. *Conservation Biology*, 9, 559–568.
https://doi.org/10.1046/j.1523-1739.1995.09061349.x
Cruz-Barraza, J.A., Carballo, J.L., Rocha-Olivares, A., Ehrlich, H. & Hog, M. (2012) Integrative taxonomy and molecular phylogeny of genus *Aplysina* (Demospongiae: Verongida) from Mexican Pacific. *PLOS ONE*, 7, e42049.
https://doi.org/10.1371/journal.pone.0042049
Dixon, J.R. (1969) Taxonomic review of the Mexican skinks of the *Eumeces brevirostris* group. *Natural History of Museum of Los Angeles County Contributions to Science*, 168, 1–30.
Drummond, A.J., Suchard, M.A., Xie, D. & Rambaut, A. (2012) Bayesian phylogenetics with BEAUti and the BEAST 1.7 *Molecular Biology and Evolution*, 29, 1969–1973.
https://doi.org/10.1093/molbev/mss075
Edgar, R.C. (2004) MUSCLE: multiple sequence alignment with high accuracy and high throughput. *Nucleic Acids Research*, 32, 1792–1797.
https://doi.org/10.1093/nar/gkh340
Feria Ortiz, M. (2011) *Filogenia morfológica y molecular del grupo de especies* Plestiodon brevirostris *(Squamata: Scincidae)*. Ph.D. Thesis, Facultad de Ciencias, UNAM, México, 147 pp.
Feria-Ortiz, M. & Garcia-Vázquez, U.O. (2012) A new species of *Plestiodon* (Squamata: Scincidae) from Sierra Madre del Sur of Guerrero, México. *Zootaxa*, 3339, 57–68.
Feria-Ortiz, M., Manríquez-Morán, N.L. & Nieto-Montes de Oca, A. (2011) Species limits based on mtDNA and morphological data in the polytypic species *Plestiodon brevirostris* (Squamata: Scincidae). *Herpetological Monographs*, 25, 25–51.
https://doi.org/10.1655/herpmonographs-d-10-00010.1
Flot, J.-F. (2010) SeqPHASE: a web tool for interconverting PHASE input/output files and FASTA sequence alignments. *Molecular Ecology Ressources*, 10, 162–166.
https://doi.org/10.1111/j.1755-0998.2009.02732.x
García-Barrios, R., Torres-Gómez, G. & Jaramillo-Monroy, F. (2008) *Las Barrancas de Cuernavaca*. CRIM-UNAM, Cuernavaca, 14 pp.
Griffith, H. (1991) Heterochrony and evolution of sexual dimorphism in the *fasciatus* group of the scincid genus *Eumeces*. *Journal of Herpetology*, 25, 24–30.
https://doi.org/10.2307/1564790
Günther, A. (1860) On new reptiles and fishes from Mexico. *Proceedings of the Zoological Society of London*, 1860, 316–318.
Heideman, N.J., Mulcahy, D.G., Sites Jr., J.W., Hendricks, M.G. & Daniels, S.R. (2011) Cryptic diversity and morphological convergence in threatened species of fossorial skinks in the genus *Scelotes* (Squamata: Scincidae) from the Western Cape Coast of South Africa: implications for species boundaries, digit reduction and conservation. *Molecular Phylogenetics and Evolution*, 61, 823–833.
https://doi.org/10.1016/j.ympev.2011.08.021
Hijmans, R.J., Cameron, S.E., Parra, J.L., Jones, P.G. & Jarvis, A. (2005) Very high resolution interpolated climate surfaces for global land areas. *International Journal of Climatology*, 25, 1965–1978.
https://doi.org/10.1002/joc.1276
Hillis, D.M. & Bull, J.J. (1993) An empirical test of bootstrapping as a method for assessing confidence in phylogenetic analysis. *Systematic Biology*, 42, 182–192.
https://doi.org/10.1093/sysbio/42.2.182
Hillis, D.M., Mable, B.K., Larson, A., Davis, S.K. & Zimmer, E.A. (1996) Nucleic acids IV: sequencing and cloning. *In*: Hillis, D.M., Moritz, C. & Mable, B.K. (Eds.), *Molecular Systematics*. Sinauer Associates, Sunderland, pp. 321–381.
Huelsenbeck, J.P. & Rannala, B. (2004) Frequentist properties of Bayesian posterior probabilities of phylogenetic trees under

simple and complex substitution models. *Systematic Biology*, 53, 904–913.
https://doi.org/10.1080/10635150490522629
Jadin, R.C., Townsend, J.H., Castoe, T.A. & Campbell, J.A. (2012) Cryptic diversity in disjunct populations of Middle American montane pitvipers: a systematic reassessment of *Cerrophidion godmani*. *Zoologica Scripta*, 41, 455–470.
https://doi.org/10.1111/j.1463-6409.2012.00547.x
Jiménez-Arcos, V.H., Calzada-Arciniega, R.A., Toscano-Flores, C., Gómez Trejo-Pérez, R. & Díaz de la Vega-Pérez, A.H. (2016) Distribution notes. *Mesoscincus altamirani* (Dugès, 1891). *Mesoamerican Herpetology*, 3, 510–511.
Köhler, G. (2012) *Color Catalogue for Field Biologists*. Herpeton, Offenbach, 49 pp.
Kurita, K., Nakamura, Y., Okamoto, T., Lin, S.-M. & Hikida, T. (2017a) Taxonomic reassessment of two subspecies of Chinese skink in Taiwan based on morphological and molecular investigations (Squamata, Scincidae). *ZooKeys*, 687, 131–148.
https://doi.org/10.3897/zookeys.687.12742
Kurita, K., Ota, H. & Hikida, T. (2017b) A new species of *Plestiodon* (Squamata: Scincidae) from the Senkaku Group, Ryukyu Archipelago, Japan. *Zootaxa*, 4254 (5), 520–536.
https://doi.org/10.11646/zootaxa.4254.5.2
Lanfear, R., Frandsen, P.B., Wright, A.M., Senfeld, T. & Calcott, B. (2016) PartitionFinder 2: new methods for selecting partitioned models of evolution for molecular and morphological phylogenetic analyses. *Molecular Biology and Evolution*, 34, 772–773.
https://doi.org/10.1093/molbev/msw260
Leaché, A.D. & Fujita, M.K. (2010) Bayesian species delimitation in West African forest geckos (*Hemidactylus fasciatus*). *Proceedings of the Royal Society B*, 277, 3071–3077.
https://doi.org/10.1098/rspb.2010.0662
Leaché, A.D. & Reeder, T.W. (2002) Molecular systematics of the Eastern Fence Lizard (*Sceloporus undulatus*): a comparison of parsimony, likelihood and Bayesian approaches. *Systematic Biology*, 51, 44–68.
https://doi.org/10.1080/106351502753475871
Lee, J.C. (2000) *A Field Guide to the Amphibians and Reptiles of the Maya World. The Lowlands of Mexico, Northern Guatemala, and Belize*. Comstock Publishing Associates, Cornell University Press, Ithaca, New York, 402 pp.
Méndoza-Hernández, A.A., Pérez-Ramos, E., Solano-Zavaleta, I. & Roth-Monzón, A.J. (2011) Extensión de la distribución geográfica de *Mesoscincus altamirani* (Squamata: Sauria: Scincidae) en el estado de Guerrero, México. *Revista Mexicana de Biodiversidad*, 82, 1049–1052.
Miller, M.A., Pfeiffer, W. & Schwartz, T. (2010) Creating the CIPRES Science Gateway for inference of large phylogenetic trees. *In*: Institute of Electrical and Electronics Engineers (IEEE) (Ed.), *Proceedings of the Gateway Computing Environments Workshop (GCE)*, 2010, New Orleans, pp. 1–8.
https://doi.org/10.1109/GCE.2010.5676129
Moen, D.S., Irschick, D.J. & Wiens, J.J. (2013) Evolutionary conservatism and convergence both lead to striking similarity in ecology, morphology and performance across continents in frogs. *Proceedings of the Royal Society of London B: Biological Sciences*, 280, 20132156.
https://doi.org/10.1098/rspb.2013.2156
Morrone, J.J. (2014) Biogeographical regionalisation of the Neotropical region. *Zootaxa*, 3782, 1–110.
https://doi.org/10.11646/zootaxa.3782.1.1
Myers, C.W. & Donnelly, M.A. (1991) The lizard genus *Sphenomorphus* (Scincidae) in Panama, with description of a new species. *American Museum Novitates*, 3027, 1–12.
Ochoa Ochoa, L.M. & Flores Villela, O.A. (2006) *Áreas de Diversidad y Endemismo de la Herpetofauna Mexicana*. Las Prensas de Ciencias, Facultad de Ciencias, UNAM, México, 211 pp.
Pavón Vázquez, C.J. (2015) *Reevaluación de los límites de especies en el escinco* Plestiodon brevirostris *con base en datos multi-locus*. M.S. Thesis, Facultad de Ciencias, UNAM, México, 116 pp.
Peters, J.A. (1954) The amphibians and reptiles of the coast and coastal sierra of Michoacán, Mexico. *Occasional Papers of the Museum of Zoology, University of Michigan*, 554, 1–37.
Pyron, R.A., Burbrink, F.T. & Wiens, J.J. (2013) A phylogeny and updated classification of Squamata, including 4161 species of lizards and snakes. *BMC Evolutionary Biology*, 13, 93.
https://doi.org/10.1186/1471-2148-13-93
Rambaut, A., Suchard, M.A., Xie, D. & Drummond, A.J. (2014) Tracer v1.6. Available from: http://beast.bio.ed.ac.uk/Tracer (accessed 29 May 2017)
Reeder, T.W. (2003) A phylogeny of the Australian *Sphenomorphus* group (Scincidae: Squamata) and the phylogenetic placement of the crocodile skinks (*Tribolonotus*): Bayesian approaches to assessing congruence and obtaining confidence in maximum likelihood inferred relationships. *Molecular Phylogenetics and Evolution*, 27, 384–397.
https://doi.org/10.1016/s1055-7903(02)00448-7
Rittmeyer, E.N. & Austin, C.C. (2017) Two new species of Crocodile Skinks (Squamata: Scincidae: *Tribolonotus*) from the Solomon Archipelago. *Zootaxa*, 4268 (1), 71–87.
https://doi.org/10.11646/zootaxa.4268.1.4
Robinson, D.M. (1979) Systematics of skinks of the Eumeces brevirostris species group in Western Mexico. *Contributions in Science, Natural History Museum of Los Angeles County*, 319, 1–13.
Rzedowski, J. (1983) *Vegetación de México*. 2nd Edition. Editorial Limusa, México, 432 pp.
Sabaj, M.H. (2016) Standard symbolic codes for institutional resource collections in herpetology and ichthyology: an online reference. Version 6.5 (16 August 2016). American Society of Ichthyologists and Herpetologists, Washington, DC. Available from: http://www.asih.org/ (accessed 8 September 2016)

Schmitz, A., Brandley, M.C., Mausfeld, P., Vences, M., Glaw, F., Nussbaum, R.A. & Reeder, T.W. (2005) Opening the black box: phylogenetics and morphological evolution of the Malagasy fossorial lizards of the subfamily "Scincinae". *Molecular Phylogenetics and Evolution*, 34, 118–133.
https://doi.org/10.1016/j.ympev.2004.08.016
Stamatakis, A. (2006) RAxML-VI-HPC: maximum likelihood-based phylogenetic analyses with thousands of taxa and mixed models. *Bioinformatics*, 22, 2688–2690.
https://doi.org/10.1093/bioinformatics/btl446
Stamatakis, A. (2014) RAxML version 8: a tool for phylogenetic analysis and post-analysis of large phylogenies. *Bioinformatics*, 30, 1312–1313.
https://doi.org/bioinformatics/btu033
Stephens, M. & Scheet, P. (2005) Accounting for decay of linkage disequilibrium in haplotype inference and missing-data imputation. *American Journal of Human Genetics*, 76, 449–462.
https://doi.org/10.1086/428594
Stephens, M., Smith, N. & Donnelly, P. (2001). A new statistical method for haplotype reconstruction from population data. *American Journal of Human Genetics*, 68, 978–989.
https://doi.org/10.1086/319501
Tamura, K., Stecher, G., Peterson, D., Filipski, A. & Kumar, S. (2013) MEGA6: Molecular Evolutionary Genetics Analysis version 6.0. *Molecular Biology and Evolution*, 30, 2725–2729.
https://doi.org/10.1093/molbev/mst197
Taylor, E.H. (1933) A new species of lizard from Mexico. *The University of Kansas Science Bulletin*, 21, 257–262.
Taylor, E.H. (1935) A taxonomic study of the cosmopolitan scincoid lizards of the genus *Eumeces* with an account of the distribution and relationships of its species. *The University of Kansas Science Bulletin*, 23, 1–643.
Townsend, T.M., Alegre, R.E., Kelley, S.T., Wiens, J.J. & Reeder, T.W. (2008) Rapid development of multiple nuclear loci for phylogenetic analysis using genomic resources: an example from squamate reptiles. *Molecular Phylogenetics and Evolution*, 47, 129–142.
https://doi.org/10.1016/j.ympev.2008.01.008
Uetz, P. (Ed.) (2016) The reptile database. Available from: http://www.reptile-database.org (accessed 8 September 2016)
Webb, R.G. (1959) *Eumeces colimensis* (Sauria, Scincidae), in Sinaloa, Mexico. *The Southwestern Naturalist*, 4, 42.
https://doi.org/10.2307/3669531
Webb, R.G. (1968) The Mexican skink *Eumeces lynxe* (Squamata, Scincidae). *Publications of the Museum, Michigan State University*, Biological Series, 4, 1–28.
Wilson, L.D., Mata-Silva, V. & Johnson, J.D. (2013) A conservation reassessment of the reptiles of Mexico based on the EVS measure. *Amphibian & Reptile Conservation*, 7, 1–47.
Yang, Z. (2015) The BPP program for species tree estimation and species delimitation. *Current Zoology*, 61, 854–865.
https://doi.org/10.1093/czoolo/61.5.854
Yang, Z. & Rannala, B. (2010) Bayesian species delimitation using multilocus sequence data. *Proceedings of the National Academy of Sciences of the United States of America*, 107, 9264–9269.
https://doi.org/10.1073/pnas.0913022107

APPENDIX I

Specimens examined. UAGro refers to specimens catalogued in the Universidad Autónoma de Guerrero, Guerrero, Mexico. ANMO, CJPV, ENS, ICS, JCBH, LNG, and UOGV are field identifiers for uncatalogued specimens being deposited in the MZFC-HE.

***Plestiodon brevirostris*: MEXICO: GUERRERO:** Crucero del Carrizal (MZFC-HE 642); 250 m NE Crucero del Carrizal (MZFC-HE 691); Omiltemi, 4 km ESE Cueva del Tigre (MZFC-HE 2851); Omiltemi, on way to Las Trincheras (MZFC-HE 2853, 2863, 2874); 2 km SE Omiltemi (MZFC-HE 2854); 1 km S Omiltemi, on way to Agua Fría (MZFC-HE 2855–2856); 2 km ESE Omiltemi (MZFC-HE 2857–2858, 2870); Omiltemi, on way to La Joya (MZFC-HE 2859, 2864); Omiltemi, Laguna Escondida (MZFC-HE 2862); Omiltemi, 2.4 km E, Plan de Potrerillos (MZFC-HE 2865); Omiltemi, Palo Hueco (MZFC-HE 2867); Omiltemi, 1.5 km S, on way to Agua Fría (MZFC-HE 2868); Omiltemi, 2 km S, cedral zone (MZFC-HE 2869); Omiltemi, 3 km E, Plan de Potrerillos (MZFC-HE 2871); Omiltemi, Plan de Potrerillos (MZFC-HE 2872); Omiltemi, Barranca de Potrerillos (MZFC-HE 2873); outskirts of Omiltemi, sawmill ruins (MZFC-HE 10182–10183, 10185–10186); 1.8 km SE Chalma, Atlixtac (MZFC-HE 12539); 2 km SE Lago Agua Fría, NW limit of Parque Estatal de Omiltemi (MZFC-HE 12933–12935); Balzamar, above Carrizal de Bravo, 17.567 N, 99.55 W (MZFC-HE 25382); Omiltemi, 17.4833 N, 99.65 W (MZFC-HE 25383); Sierra de Alquitrán, near Chilpancingo to the W, 17.5 N, 99.467 W (MZFC-HE 25384); 2 km S Chalma, Atlixtac, 17.48467 N, 98.8864722 W (ANMO 3345); near Chalma, Atlixtac, 17.493167 N, 98.8683611 W (ANMO 3563); ca. 0.5 km Chalma towards Tlatlauquitepec, 17.493167 N, 98.8683611 W (ANMO 3564–3566, 3568, 3574–3575); ca. 0.5 km Chalma towards Tlatlauquitepec, 17.49625 N, 98.8665833 W (ANMO 3567); 2.75 km (in straight line) NW Cabecera Municipal de Metlaltónoc, Cochoapa el Grande, 17.20567 N, 98.43111 W (ANMO 3901–3902); **OAXACA:** 0.8 mi S on road to Morelos, 17.1056 N, 97.70611 W (MZFC-HE 441–444); Sierra Juárez, Mitla-Totontepec road, 11.9 mi S Totontepec (MZFC-HE 5309–5310); Sierra de Juárez, ca. 5 km E Santiago Comaltepec, 17.5667 N, 96.51667 W (MZFC-HE 1102); Teotitlán del Valle road, just below Benito Juárez (MZFC-HE 1161–1162); base of Cerro Piedra Larga, towards Tehuantepec Isthmus, 16.585 N, 95.801389 W (MZFC-HE 8738); high portions of Zoquiápam Boca de los Ríos, Sierra Monteflor, 17.550278 N, 96.733611 W (MZFC-HE 8739); Cerro Yucunino, 7.5 km SE Llano de Guadalupe 17.1507167 N, 97.6213 W

(MZFC-HE 13446); E Morelos (MZFC-HE 13448–13449); Santo Tomas Teipan (MZFC-HE 15568); Mitla, 16.9841944 N, 96.3348056 W (MZFC-HE 19134); El Punto, Sierra de Juárez (MZFC-HE 21013); Santa María Yavesía, 17.22 N, 96.4356 W (MZFC-HE 24472–24474); 2 km from road Ixtlán-San Pablo Macuiltianguis, 17.55 N, 96.55 W (MZFC-HE 25385–25386); Santa Inés del Monte, Zaachila, 16.93278 N, 96.866389 W (MZFC-HE 25387–25389, 25539); 14 mi NE Díaz Ordaz, 16.074167 N, 96.396389 W (MZFC-HE 25390); Cerro San Felipe (MZFC-HE 25392); Teotitlán del Valle-Benito Juárez road, 17.1033 N, 96.49833 W (MZFC-HE 25393); 4 km SE San Isidro Buenos Aires, 17.938056 N, 96.865278 W (MZFC-HE 25538; ANMO 3995–3998, 4009); ca. 2km SE Santiago Comaltepec, on dirt road to road MX176, 17.55819 N, 96.53721 W (MZFC-HE 27173, 27179); La Unión Altamira Monteverde, Santa Lucía Monteverde, Putla, 16.994767 N, 97.7010833 W (ANMO 822); 2.7 km S La Puerta del Sol, 17.5136 N, 96.5159 W (ICS 431); **PUEBLA:** 3–5 km E Azumbilla, 18.6722 N, 97.36167 W (MZFC-HE 721–722); Acajete (MZFC-HE 3139); Sierra Negra, microwave station, 18.321 N, 97.057 W (MZFC-HE 16472); vicinities of Zoquitlán, 18.322 N, 97.013 W (MZFC-HE 16480); San Miguel Calixitla, 19.2643056 N, 97.19811 W (MZFC-HE 25347–25350); Zoquitlán, microwave station, 18.32322 N, 97.05688 W (ANMO 3948); Zoquitlán, on way to river, 18.329893 N, 97.007347 W (ANMO 3953–3955); Zoquitlán-Coyomeapan road, 18.30268 N, 96.99699 W (ANMO 4226–4227); San Juán del Valle town, ca. 1 km S of town, 19.25625 N, 97.198278 W (CJPV 2–3); near Totalco (El Limón), 19.48145 N, 97.35079 W (UOGV 2607–2612); **TLAXCALA:** turnoff to Españita, road 138 (MZFC-HE 21150); Cerro Tecoae, ca. 12 km N Huamantla, 19.39122 N, 97.921639 W (MZFC-HE 25343–25345); 8.5 km NW Benito Juárez, after Ranchería Torres, 2.4 km. N Huamantla, 19.4402 N, 97.88258 W (MZFC-HE 26310–26314, 26316); San Antonio, San Juan Ixtenco (ANMO 1895).

***Plestiodon copei*: MEXICO: CIUDAD DE MÉXICO:** Ajusco, Monte Alegre, Tlalpan (MZFC-HE 179–180); El Capulín, Tlalpan (MZFC-HE 183, 571, 3269 (1, 3–5, 7–8, 10–11, 13, 19–28)); Ajusco, Tlalpan (MZFC-HE 852); Ajusco, Tlalpan, 19.20667 N, 99.25833 W (MZFC-HE 4694 (1–2)); Ejido San Nicolás Totolapan, 2 Km W Albergue Alpino, Monte Alegre zone, Magdalena Contreras (MZFC-HE 11678); Ejido San Nicolás Totolapan, Magdalena Contreras, 19.25281 N, 99.32008 W (MZFC-HE 23585); Ejido San Nicolás Totolapan, Magdalena Contreras, 19.25444 N, 99.31811 W (MZFC-HE 23586–23587); Paraje El Aguaje, Magdalena Contreras (MZFC-HE 23965); Cieneguillas, Cuajimalpa, 19.24186 N, 99.3295 W (MZFC-HE 24031); 1.7 km ENE tower of Cerro San Miguel, very close to Paraje El Mirador, Cuajimalpa, (MZFC-HE 24070); tower of Cerro San Miguel, Desierto de los Leones, 19.26743 N, 99.32193 W (MZFC-HE 25462–25466); Magdalena Contreras (MZFC-HE 29755–29756); **MÉXICO:** 3 km SW Los Llorones (MZFC-HE 315–316); San Cayetano, game breeding place (MZFC-HE 514); El Capulín (MZFC-HE 570 (1–3)); Cerro Telapon, western slope (MZFC-HE 915); Parque Nacional Zoquiapan, 19.305 N, 98.72167 W (MZFC-HE 3208 (1–2)); Parque Nacional Miguel Hidalgo (MZFC-HE 3312 (1–2)); Cerro Tepalcates, Parque Nacional Miguel Hidalgo (MZFC-HE 5450); Piedra Grande, 19.35023 N, 99.39557 W (MZFC-HE 17968); Piedra Grande, 19.34965 N, 99.39558 W (MZFC-HE 25412); **MICHOACÁN:** Cerro Burro, microwave station, 18.55 N, 103.30333 W (MZFC-HE 6046 (1–2)); **MORELOS:** Huitzilac-Lagunas de Zempoala road, 19.04392 N, 99.30333 W (MZFC-HE 29701–29704); **PUEBLA:** Campo Experimental San Juan Tetla (MZFC-HE 14113); **TLAXCALA:** Huilo, Piedra Agujerada (MZFC-HE 16863).

***Plestiodon indubitus*: MEXICO: CIUDAD DE MÉXICO:** El Capulín, Tlalpan (MZFC-HE 3269 (9, 12)); **GUERRERO:** Taxco-Ixcateopan road, km 26.5 (MZFC-HE 3920); Ixcateopan de Cuauhtémoc, W Barranca (MZFC-HE 3921); 2km E Ixcateopan de Cuauhtémoc (MZFC-HE 3923, 3927); Taxco-Ixcateopan road, km 8 (MZFC-HE 3924); San Miguel, Taxco (MZFC-HE 3925); Pedro Ascencio Alquisiras, 200 m SW Cruz Alta (MZFC-HE 3926); 2 km SE Las Peñas, Ixcateopan (MZFC-HE 3928); Landa, beside Taxco, 18.55972 N, 99.62889 W (MZFC-HE 25471); **MÉXICO:** 5 km E Pipioltepec (MZFC-HE 307); Ocuilán, Tlaltizapan, on Cuernavaca-Chalma dirt road (MZFC-HE 11796); Rancho La Mecedora, on way to Peña Blanca, Avándaro, Valle de Bravo (MZFC-HE 11798); Valle de Bravo (MZFC-HE 25414–25415); **MORELOS:** 0.5 km W Coajomulco (MZFC-HE 3334); 1.8 km W Huitzilac, road 95, between Tres Marías and Zempoala (MZFC-HE 11189); Chichinautzin lava field (MZFC-HE 24668); Tepoztlán (MZFC-HE 25417–25420, 25443–25444); ca. 2 km S Tres Marías, km 56 of Tres Marías-Cuernavaca road, 19.02923 N, 99.21968 W (MZFC-HE 25460, 25469); km. 61 of Tres Marías-Cuernavaca road, 19.01173 N, 99.23527 W (MZFC-HE 25461, 25470); ca. 1 km N Huitzilac, 19.02378 N, 99.28047 W (MZFC-HE 25468); ca. 1 km N Biomédicas UAEM, Cuernavaca (MZFC-HE 25472–25473); 8 km S Tres Marías, 19.02022 N, 99.21447 W (UOGV 2524).

***Plestiodon lynxe lynxe*: MEXICO: HIDALGO:** 0.5 km E Tejocotal (MZFC-HE 177); Mineral del Chico and La Presa (MZFC-HE 3302, 3318); Pueblo Nuevo, El Chico, 20.17166 N, 98.69667 W (MZFC-HE 3313 (1–3)); Parque Nacional El Chico, Cruz de los Negros (MZFC-HE 3317-1–3317-3); La Mojonera (MZFC-HE 5398); La Hojarasca (MZFC-HE 5463 (1–2)); turnoff for San Vicente on Highway 85, W of Jacala (MZFC-HE 11200); 2.5 km S Agua Zarca, on road to Tenango de Doria, N of Hueytlalpan and Tulancingo, 20.331 N, 98.30717 W (MZFC-HE 16038); Zoquizoquiapan (MZFC-HE 20623–20624); Palo Gacho (MZFC-HE 21146); 1.5 km W Eloxochitlán (MZFC-HE 21147); Chichiuaixtle River (MZFC-HE 21149); Zietla, near Tres Cruces (MZFC-HE 21151); Aguacatitla, 21.07533 N, 98.53817 W (MZFC-HE 23098); **PUEBLA:** 10 km S Huauchinango (MZFC-HE 3233); 13.8 km SE Chignahuapan, towards Tetela (MZFC-HE 3450); 24 km S Chignahuapan, towards Apizaco (MZFC-HE 3451–3452); Chignahuapan, turnoff for Composela (MZFC-HE 3531); stream 10 km S of Chignahuapan (MZFC-HE 4795–4796); 9 km E Tetela, on road (MZFC-HE 4820 (1–3)); 15 mi S Ahuazotepec, Road 119, 19.86083 N, 97.76083 W (MZFC-HE 5169); Los Azufres, southern slope, 2 km W Cruz Colorada (MZFC-HE 11573–11575); Huaxtla, 19.84097 N, 97.51436 W (MZFC-HE 20610); Ocotlán de Betancourt, 19.80219 N, 97.54711 W (MZFC-HE 22737); Gómez Poniente, 19.763 N, 97.49308 W (MZFC-HE 22738); Huaxtla, 19.84292 N, 97.51469 W (MZFC-HE 22739); Huaxtla, 19.84178 N, 97.51453 W (MZFC-HE 22746); **QUERÉTARO:** Pinal de Amoles, 21.135 N, 99.625 W (MZFC-HE 336 (1–6)); Puerta del Cielo, Pinal de Amoles (MZFC-HE 6150); Pinal de Amoles, Rancho Nuevo (MZFC-HE 6923); ca. 2 km NE El Doctor, towards Cerro Tecolote, 20.85111 N, 99.58722 W (MZFC-HE 8404–8405); 7 km SE Tres Lagunas, 21.29667 N, 99.17944 W (MZFC-HE 9144–9158, 9164); 6 Km NW Rancho Los Velázquez, towards San Gaspar, 21.13278 N, 99.69167 W (MZFC-HE 9159–9163); ca. 2.5 km NE El Madroño by road to Valle Guadalupe, 21.28611 N, 99.17861 W (MZFC-HE 9310);

Pinal de Zamorano, 20.92833 N, 100.18056 W (MZFC-HE 9391–9392); Pinal de Zamorano, 20.93250 N, 100.18 W (MZFC-HE 9393–9397, 9400); Pinal de Zamorano, 20.92361 N, 100.17389 W (MZFC-HE 9398–9399); 1 km S turnoff to El Doctor, 20.85361 N, 99.61083 W (MZFC-HE 9786); San Joaquín, 20.93322 N, 99.59142 W (MZFC-HE 17839–17840); Pinal del Zamorano (MZFC-HE 21148); 1 km S Pinal de Amoles (MZFC-HE 21292); 2 km N Los Trigos, towards Cerro El Zamorano (MZFC-HE 24628–24629); Sierra Gorda, near summit of Cerro Grande, western slope, 21.43331 N, 99.13644 W (MZFC-HE 27707); **SAN LUSI POTOSÍ:** 2 km W Álvarez, 22.03194 N, 100.615 W (MZFC-HE 11083); **TLAXCALA:** Tlaxco (MZFC-HE 3190); **VERACRUZ:** San Sebastián, 10 km NW Nautla (MZFC-HE 178).

***Plestiodon nietoi*: MEXICO: GUERRERO:** El Filo, El Balcón, 17.58153 N, 100.54878 W (MZFC-HE 22247–22248); La Llave, El Balcón, Ajuchitán del Progreso, 17.62275 N, 100.57481 W (MZFC-HE 22249–22252); El Moreno, El Balcón, 17.58153 N, 100.54878 W (MZFC-HE 22253–22254); La Ola-San Antonio de las Texas road, 17.68907 N, 100.8721 (UTA-R 58460–58464; ENS 11530).

***Plestiodon ochoterenae*: MEXICO: GUERRERO:** Agua de Obispo, 17.32328 N, 99.47228 W (MZFC-HE 25454); Agua de Obispo, 17.32192 N, 99.47006 W (MZFC-HE 25467); Palo Blanco, Chilpancingo (UAGro, 2 specimens); Guerrero (JCBH 255); road to Chichihualco from Chilpancingo, ca. 25 km E of Chichihualco, 17.61264 N, 99.56692 W (LNG 159); **OAXACA:** San Vicente, Putla District (UCM 52640).

***Plestiodon sumichrasti*: MEXICO: OAXACA:** San Isidro la Gringa, 17.09494 N, 94.11933 W (MZFC-HE 18652–18653, 18661, 18666); Chalchijapa, 17.05416 N, 94.65388 W (MZFC-HE 18654–18660, 18662–18665); Ejido San Francisco La Paz, 17.07889 N, 94.1125 W (MZFC-HE 20547); **VERACRUZ:** Los Tuxtlas, Santa Martha (MZFC-HE 4681); Sierra Santa Martha, Los Tuxtlas (MZFC-HE 5577); San Andrés Tuxtla (MZFC-HE 7613); Cacahuatal, Ixhuatlán del Café (MZFC-HE 25413); Arroyo Zarco, Uxpanapa, 17.20556 N, 94.48461 W (MZFC-HE 29426).

SUPPLEMENTARY TABLE 1. Characters recorded in all the available specimens from the Balsas Basin. For scutellation characters, an asterisk (*) indicates that they are meristic (i.e., the number of scales was counted) and a plus sign ($^+$) that they are binary (i.e., the presence or absence of each character was recorded).

Type of character	Character
Scutellation$^+$	Frontonasal-frontal contact
Scutellation*	Supraoculars
Scutellation*	Supraoculars contacting frontal
Scutellation*	Nuchals
Scutellation$^+$	Upper presubocular-third supralabial contact
Scutellation*	Superciliaries
Scutellation*	Postsuboculars
Scutellation*	Postsuboculars contacting sixth supralabial
Scutellation$^+$	Upper postsubocular-upper secondary temporal contact
Scutellation$^+$	Primary temporal
Scutellation$^+$	Upper secondary temporal-seventh supralabial contact
Scutellation*	Scales contacting upper secondary temporal between upper postsubocular and first nuchal
Scutellation*	Postlabials
Scutellation*	Scales contacting both upper secondary temporal and upper postlabial
Scutellation*	Scales as large as, or larger than, upper postlabial contacting it
Scutellation$^+$	Wider than long scale bordering the postgenial medially
Scutellation*	Transverse dorsal scale rows between nuchals and level above vent
Scutellation*	Longitudinal dorsal scale rows around midbody
Scutellation*	Lamellae under fourth toe
Morphometric	Snout-vent length (SVL)
Morphometric	Head length
Morphometric	Trunk length
Morphometric	Tibia length
Coloration	Posterior extent of upper secondary dark line
Coloration	Posterior extent of dorsolateral light line
Coloration	Dorsal extent of dorsolateral light line (at levels of midneck and midbody)
Coloration	Posterior extent of lateral light line
Coloration	Dorsal extent of lateral light line (at level of midneck)

SUPPLEMENTARY TABLE 2. Specimens included in the molecular analyses. Samples arranged by taxon name and voucher number, in that order. All specimens from Mexico except for a sample of *P. laticeps*. GB accession numbers are given for the sequences of each locus.

ID	Taxon	Voucher	Locality	*ND1*	*MKL1*	*R35*
1	*Plestiodon bilineatus*	MZFC-HE 25338	Ejido Chavarría Viejo, Durango (23.7152 N, 105.48682 W)	HQ655824	MF615444	MF615454
2	*P. bilineatus*	MZFC-HE 25340	Ejido Chavarría Viejo, Durango (23.7152 N, 105.48682 W)	HQ655825	HM160698	HM161072
3	*P. bilineatus*	MZFC-HE 25341	Balleza, Chihuahua (26.48995 N, 106.36355 W)	HQ655822	HM160697	HM161071
4	*P. bilineatus*	MZFC-HE 25342	Santiago Papasquiaro, Durango (25.07422 N, 105.62873 W)	HQ655823	–	–
5	*P. bilineatus*	MZFC-HE 25536	Balleza, Chihuahua (26.48995 N, 106.36355 W)	HQ655821	–	–
6	*P. bilineatus*	MZFC-HE 25537	Las Crucitas, Zacatecas (22.9375 N, 103.53778 W)	HQ655826	–	–
7	*P. bilineatus*	UTA-R 52706	Highway Bolaños-Tuxpan de Bolaños, Jalisco	HQ655828	–	–
8	*P. bilineatus*	UTA-R 53300	Highway Bolaños-Tuxpan de Bolaños, Jalisco	HQ655827	–	–
9	*P. brevirostris*	MZFC-HE 15568	Santo Tomás Teipan, Oaxaca	HQ655833	–	–
10	*P. brevirostris*	MZFC-HE 25343	Cerro Tecoae, Tlaxcala (19.39122 N, 97.921639 W)	HQ655830	HM160699	HM161073
11	*P. brevirostris*	MZFC-HE 25344	Cerro Tecoae, Tlaxcala (19.39122 N, 97.921639 W)	HQ655831	–	–
12	*P. brevirostris*	MZFC-HE 25346	El Seco, Puebla (19.13611 N, 97.64056 W)	HQ655829	MF615445	MF615455
13	*P. brevirostris*	MZFC-HE 25382	Balzamar, Guerrero (17.567 N, 99.55 W)	HQ655838	MF615447	MF615457
14	*P. brevirostris*	MZFC-HE 25383	Omiltemi, Guerrero (17.4833 N, 99.65 W)	HQ655840	–	–
15	*P. brevirostris*	MZFC-HE 25384	Sierra de Alquitrán, Guerrero (17.5 N, 99.467 W)	HQ655839	–	–
16	*P. brevirostris*	MZFC-HE 25385	2 km from road Ixtlán-San Pablo Macuiltianguis, Oaxaca (17.55 N, 96.55 W)	HQ655834	MF615448	MF615458
17	*P. brevirostris*	MZFC-HE 25386	2 km from road Ixtlán-San Pablo Macuiltianguis, Oaxaca (17.55 N, 96.55 W)	HQ655835	HM160700	HM161074
18	*P. brevirostris*	MZFC-HE 25390	14 mi NE Díaz Ordaz, Oaxaca (16.07417 N, 96.39639 W)	HQ655832	–	–
19	*P. brevirostris*	MZFC-HE 25538	4 km SE San Isidro Buenos Aires, Oaxaca (17.938056 N, 96.865278 W)	HQ655836	–	–
20	*P. brevirostris*	MZFC-HE 25539	Santa Inés del Monte, Oaxaca (16.93278 N, 96.866389 W)	HQ655837	–	–
21	*P. copei*	MVZ 143455	1 mi W Río Frío on old road to Puebla, México (19.33778 N, 98.67611 W)	HM160803	HM160709	HM161086
22	*P. copei*	MZFC-HE 14113	Campo Experimental San Juan Tetla, Puebla	HQ655859	–	–
23	*P. copei*	MZFC-HE 25462	Desierto de los Leones, Ciudad de México (19.26743 N, 99.32193 W)	HQ655860	HM160708	HM161085
24	*P. dicei*	MZFC-HE 18763	Ejido La Cima, Tamaulipas (23.05814 N, 99.19375 W)	HM160804	HM160710	HM161087
25	*P. dicei*	MZFC-HE 18764	Ejido La Cima, Tamaulipas (23.05814 N, 99.19375 W)	HQ655846	–	–
26	*P. dicei*	MZFC-HE 18767	1 km E Marmolejo, Tamaulipas (24.62217 N, 99.03194 W)	HQ655841	–	–
27	*P. dicei*	MZFC-HE 18768	1 km E Marmolejo, Tamaulipas (24.62217 N, 99.03194 W)	HQ655842	–	–
28	*P. dicei*	MZFC-HE 25353	Parque Ecológico Chipinqué, Nuevo León (25.61403 N, 100.35417 W)	HQ655845	–	–
29	*P. dicei*	MZFC-HE 25356	Rancho El Manzano, Nuevo León (25.35233 N, 100.19333 W)	HQ655843	HM160711	HM161088
30	*P. dicei*	MZFC-HE 25359	Rancho El Manzano, Nuevo León (25.35233 N, 100.19333 W)	HQ655844	–	–
31	*P. dicei*	MZFC-HE 25366	Los Lirios, Coahuila (25.37569 N, 100.51081 W)	HQ655858	MF615446	MF615456
32	*P. dugesii*	MCB 1054	Queréndaro, Michoacán (19.68612 N, 100.87945 W)	HM160807	HM160713	HM161090
33	*P. dugesii*	MZFC-HE 25327	Rancho Los Lobos, Michoacán (19.39139 N, 102.17361 W)	HQ655861	–	–

……continued on the next page

SUPPLEMENTARY TABLE 2. (Continued)

ID	Taxon	Voucher	Locality	*ND1*	*MKL1*	*R35*
34	*P. dugesii*	MZFC-HE 25328	Rancho Los Lobos, Michoacán (19.39139 N, 102.17361 W)	HQ655862	–	–
35	*P. dugesii*	MZFC-HE 25331	ca. 3 km S Atemajac de Brizuela, Jalisco	HQ655863	HM160746	HM161123
36	*P. indubitus*	MZCF-HE 25443	Tepoztlán, Morelos	HQ655847	MF615449	MF615459
37	*P. indubitus*	MZCF-HE 25460	ca. 2 km S Tres Marías, Morelos (19.02923 N, 99.21968 W)	HQ655852	–	–
38	*P. indubitus*	MZCF-HE 25461	Km. 61 of Tres Marías-Cuernavaca road, Morelos (19.01173 N, 99.23527 W)	HQ655853	–	–
39	*P. indubitus*	MZCF-HE 25468	ca. 1 km N Huitzilac, Morelos (19.02378 N, 99.28047 W)	HQ655857	HM160702	HM161076
40	*P. indubitus*	MZCF-HE 25469	ca. 2 km S Tres Marías, Morelos (19.02923 N, 99.21968 W)	HQ655851	–	–
41	*P. indubitus*	MZCF-HE 25470	Km. 61 of Tres Marías-Cuernavaca road, Morelos (19.01173 N, 99.23527 W)	HQ655854	–	–
42	*P. indubitus*	MZFC-HE 25471	Landa, Guerrero (18.55972 N, 99.62889 W)	HQ655848	–	–
43	*P. indubitus*	MZCF-HE 25472	ca. 1 km N Biomédicas UAEM, Morelos	HQ655855	–	–
44	*P. indubitus*	MZCF-HE 25473	ca. 1 km N Biomédicas UAEM, Morelos	HQ655856	–	–
45	*P. laticeps*	CAS 218689	Liberty Co., Florida, USA (30.05889 N, 84.94722 W)	HM160824	HM160730	HM161107
46	*P. lynxe lynxe*	LSUMZ-H 14823	San Luis Potosí	HM160829	HM160735	HM161112
47	*P. lynxe lynxe*	LSUMZ-H 14966	Hidalgo	HM160830	HM160736	HM161113
48	*P. lynxe lynxe*	MZFC-HE 17839	San Joaquín, Querétaro (20.93322 N, 99.59142 W)	HQ655870	–	–
49	*P. lynxe lynxe*	MZFC-HE 17840	San Joaquín, Querétaro (20.93322 N, 99.59142 W)	HQ655871	–	–
50	*P. ochoterenae*	MZFC-HE 25454	Agua de Obispo, Guerrero (17.32328 N, 99.47228 W)	HQ655865	HM160745	HM161122
51	*P. ochoterenae*	MZFC-HE 25467	Agua de Obispo, Guerrero (17.32192 N, 99.47006 W)	HQ655864	HM160744	HM161121
52	*P. parviauriculatus*	MZFC-HE 25394	4 km E Ubalama, Sonora (26.99343 N, 108.9754 W)	HQ655866	–	–
53	*P. parviauriculatus*	MZFC-HE 25395	4 km E Ubalama, Sonora (26.99343 N, 108.9754 W)	HQ655867	HM160746	HM161123
54	*P. parvulus*	MZFC-HE 25367	Pueblo Nuevo (on road 200 La Placita-Manzanillo), Michoacán (18.5613 N, 103.594367 W)	HM160841	HM160747	HM161124
55	*P. parvulus*	MZFC-HE 25370	ca. 1.4–2.4 km E La Central, Colima (19.149 N, 104.42647 W)	HQ655868	–	–
56	*P. parvulus*	MZFC-HE 25371	ca. 1.4–2.4 km E La Central, Colima (19.149 N, 104.42647 W)	HQ655869	–	–
57	*P. sumichrasti*	MZFC-HE 25413	Ixhuatlán del Café, Veracruz	HM160852	HM160758	HM161134
58	*P. tetragrammus*	MZFC-HE 18766	1 km E Marmolejo, Tamaulipas (24.62217 N, 99.03194 W)	HM160855	HM160761	HM161137
59	*Plestiodon* sp. Balsas	MZFC-HE 19787	Cañada El Limón, Guerrero (18.19444 N, 100.16722 W)	MF615433	MF615440	MF615450
60	*Plestiodon* sp. Balsas	MZFC-HE 30620	2.7 km N Xixila, Guerrero (17.96694 N, 98.84389 W)	MF615434	MF615441	MF615451
61	*Plestiodon* sp. Balsas	MZFC-HE 30621	5.6 km N Xixila, Guerrero (17.995 N, 98.84222 W)	MF615435	–	–
62	*Plestiodon* sp. Balsas	MZFC-HE 30622	Sierra de Huautla, Morelos (18.55722 N, 98.94528 W)	MF615436	–	–
63	*Plestiodon* sp. Balsas	MZFC-HE 30623	5 km NE Santiago Tamazola, Oaxaca (17.71278 N, 98.20611 W)	MF615437	MF615442	MF615452
64	*Plestiodon* sp. Balsas	MZFC-HE 30624	5.3–5.4 km N Xixila, Guerrero (17.99333 N, 98.85056 W)	MF615438	MF615443	MF615453
65	*Plestiodon* sp. Balsas	MZFC-HE 30626	5.3–5.4 km N Xixila, Guerrero (17.99278 N, 98.85111 W)	MF615439	–	–
66	*Plestiodon* sp. Colima-Jalisco	MZFC-HE 25449	Loma del Cuervo, Jalisco (19.61689 N, 103.56031 W)	HQ655849	HM160701	HM161075
67	*Plestiodon* sp. Colima-Jalisco	MZFC-HE 25451	Loma del Cuervo, Jalisco (19.61689 N, 103.56031 W)	HQ655850	–	–